TRANSIENT AND INVERSE RESPONSE OF A HIGHLY CONDUCTING PERMEABLE SPHERE

A Thesis

Presented to

The Faculty of Graduate Studies

The University of Manitoba

In partial fulfillment

of the requirements for the degree of

MASTER OF ENGINEERING

in

ELECTRICAL ENGINEERING

By

ABDELRAZIK A.M. SEPAK

September, 1981

TRANSIENT AND INVERSE RESPONSE OF A HIGHLY CONDUCTING PERMEABLE SPHERE

BY

ABDELRAZIK A.M. SEPAK

A thesis submitted to the Faculty of Graduate Studies of the University of Manitoba in partial fulfillment of the requirements of the degree of

MASTER OF ENGINEERING

ABSTRACT

The problem of the scattered near field of a sphere excited by a uniform current loop is determined using impedance boundary condition (IBC) both in the frequency and the time domains. Approximate expressions for the scattered fields at low frequency are derived by using proper approximation to the Bessel and the Hankel functions. Simplified expressions are obtained for both plane wave and dipole excitations.

For an impedance sphere, the relationship between the response waveforms and the physical properties of the sphere is discussed. A simple approach for determination of the sphere radius and its electrical properties from the knowledge of the scattered field waveform is developed.

ACKNOWLEDGEMENTS

The author is deeply indebted to Dr. L. Shafai for the guidance and assistance (academic and physical) he graciously offered throughout the duration of this study.

Sincere gratitude is also extended to my mother who has always impressed the value of education on her children.

TABLE OF CONTENTS

LIST OF FIGURES

LIST OF MOST USED SYMBOLS

a	radius of sphere
A_r	radial component of the magnetic vector potential
A	real part of the surface impedance
E_θ	θ component of the electric field
F_r	radial component of the electric vector potential
$F(t)$	time response
f_o	fundamental frequency
H_θ	θ component of the magnetic field
$\hat{H}_n^{(2)}$	second kind spherical Hankel function of Riccati type of order n
$\hat{J}_n$	spherical Bessel function of Riccati type of order n
K	wave number of free space
$P_n^{(1)}$	associated Legendre function of the first kind of order n
Z_o	intrinsic impedance of free space
Z	surface impedance of the scatterer
Δ	normalized surface impedance (Z/Z_o)
ε_o	permittivity of free space
σ	conductivity of scatterer
μ_o	permeability of free space
μ	permeability of scatterer
λ	wavelength in free space
ω	angular frequency

CHAPTER ONE

INTRODUCTION

1.1 Literature Survey

A classical problem of practical importance is the calculation of the scattered fields resulting from a plane wave incident on a permeable sphere of finite conductivity. The results depend on the material as well as the electrical properties of the scatterer. The traditional method to attack the problem of scattering by a sphere in the frequency domain is to expand the incident plane wave field in spherical functions presented by Stratton [1] .

The problem of scattering of electromagnetic waves from a sphere with an impedance boundary condition has been discussed by various investigators. The concept of a surface impedance is, of course, not new, and has long been used in varieties of electromagnetic wave calculations. During the 1940's, a considerable number of Russian papers were published; and an attempt was made to take into account the electrical properties of the ground by specifying an impedance boundary condition at its surface. This boundary condition is usually attributed to Leontovich and was described by himself in 1948.

The Leontovich or impedance boundary condition can be written as (at the surface of the body)

$$E - (\hat{n} \cdot E)\hat{n} = Z\, \hat{n} \times H \qquad (1.1)$$

where $\hat{n}$ is a unit vector representing outward normal to the surface and E, H are the total electric and magnetic fields respectively, on the surface of the body. The quantity Z is the surface impedance of

the body, designated as the Leontovich impedance and is given by (for time dependent $e^{i\omega t}$)

$$Z = \sqrt{\frac{i\omega\mu}{i\omega\varepsilon + \sigma}} \tag{1.2}$$

where μ and ε represent the permeability and the permittivity of the body material, respectively, and σ represents the conductivity of the body.

Calculations of the far-zone scattered fields by using an impedance boundary condition in the frequency domain has been considered by Garbacz [2], Wait [3,4], Senior [5], and Mitzner [6] . Garbacz has investigated a special case of bistatic scattering from a class of lossy dielectric spheres and has derived expressions for the bistatic cross sections of these spheres. Using the same approach, Wait [4] studied the problem of scattering from spheres assuming various surface impedance boundary conditions.

Senior has discussed the validity of using impedance boundary conditions and has shown that the method is valid for surfaces whose radii of curvature are large compared with the penetration depth and for inhomogeneous materials whose properties vary slowly from point to point. Mitzner has discussed the problem of scattering from a body of finite conductivity by the formulation of two coupled integral equations relating the effective electric and magnetic surface currents. These equations were derived under the same assumptions as those of Leontovich.

In general, the scattering of electromagnetic waves from a sphere in the frequency domain has received considerable attention, due

to the fact that a rigorous solution has been known for a long time. In recent years the time domain approach to electromagnetic scattering has received considerable attention from many researchers in the field. The first attempts for deriving time domain solutions to scattering problems date back to several years ago. Kennaugh and Cosgriff [10] employed the physical optics approximation to calculate the back scattered impulse response of a rectangular flat plate, a sphere, and a spheroid. They assumed that the scatterer is a perfectly conducting body. They improved their approximate low frequency results by requiring that those results satisfy the so-called moment conditions. Weston [12] used the Inverse Laplace Transform of the back-scattered field to express the pulse returned from a perfectly conducting sphere. The inverse transform was calculated for the initial part of the pulse returned using the Tauberian theorem, while for the latter part was given exactly in terms of residues representing the natural oscillations of spheres. Rhenstein [13] described a technique based upon the Fourier Transformation of the frequency domain solution and computed the short pulse response of a perfectly conducting sphere. Additional work in time domain calculations of transient electromagnetic fields has been reported by Felsen [15] .

In summary, there are two independent techniques available for solving transient electromagnetic problems. The first of these involves the computation of the frequency domain response of the structure, which is subsequently Fourier transformed to yield the desired time domain response. The second technique is based on a direct formulation of an integral equation in the time domain and its subsequent solution.

1.2 The Problem

The scattering problems considered in this thesis are plane wave and dipole excitations illuminating a highly conducting permeable sphere both in the frequency and the time domains. The solution is based on an impedance boundary condition. For homogeneous, highly conducting permeable spheres a simple expression at low frequency for the scattered field is derived. The objective of this work is to develop a simple numerical method which can be used to study the time response of any arbitrary object.

In Chapter Two of this thesis, an approximate expression for the scattered far field from an impedance sphere at low frequency is derived. The utilization of this expression as an application for spherical target identification is discussed in detail in Chapter Five. It is found that the impedance boundary condition methods gives good accuracy compared with the classical methods used before. An approximate expression is given in a simple form for the near field at low frequencies. It is assumed that a loop excitation at low frequencies, can be replaced by a magnetic dipole at its centre. The excitation waveform is a pulse train of fundamental frequency $f_0 = 500$ Hz , with 50% duty cycle. (Experimental data for the near scattered field is available for such excitation from the Defence Research Establishment Suffield.)

Chapter Four considers the time response of a highly conducting permeable sphere with the above type of excitation. A simple approach is introduced where the time response of an impedance sphere is represented in the form of a series of complex exponentials. The coefficients of this expansion are obtained from the frequency domain

analysis of Chapter Three. In this approach which uses the surface impedance boundary condition, the time response depends only on the surface properties of the scatterer. The approach can be applied to any arbitrary object.

Chapter Five presents examples of the application of this method in both the frequency and the time domains. It is hoped that this chapter provides enough information concerning the application of waveform response to the prediction of the target identification. In this chapter the low frequency approximation is applied in both the frequency and the time domains to recover the unknown parameters of a spherical target, such as size, electrical properties, and the distance between the target centre and the excitation point, from the knowledge of the scattered field.

The ideas presented in this work are summarized in Chapter Six which also list the contribution resulting from the present study. New problems arising out of this work are pointed out and some suggestions are made for their possible solution.

CHAPTER TWO

FAR FIELD SCATTERED BY AN IMPEDANCE SPHERE

2.1 Introduction

The computation of the electromagnetic scattered fields by a class of impedance spheres, as demonstrated by Garbacz [2] and Wait [3, 4] , has stimulated considerable interest in the study of the methods based on Impedance Boundary Conditions (IBC) . One restriction inherent in the use of the surface impedance method is the requirement that $|Z/Z_o| << 1$, where Z is the surface impedance of the scatterer and Z_o is the intrinsic impedance of free space [7]. From another point of view, one of the requirements for validity of the surface impedance boundary condition is that the radii of the body be large compared to δ , the skin depth.

In the following sections the far-scattered field from an impedance sphere is determined using this method. For a plane wave incidence comparison between the IBC and the exact solutions is then presented for a lossy dielectric sphere.

2.2 Plane Wave Incidence

It is the purpose of this section to present the solution based on IBC for plane wave scattering from an impedance sphere.

2.2.1 Geometry

The geometry of the problem is defined in terms of spherical coordinates (r , θ, ϕ) and cartesian coordinates (x, y, z) with common origin and common polar axis, as indicated in Fig. 2.1. The

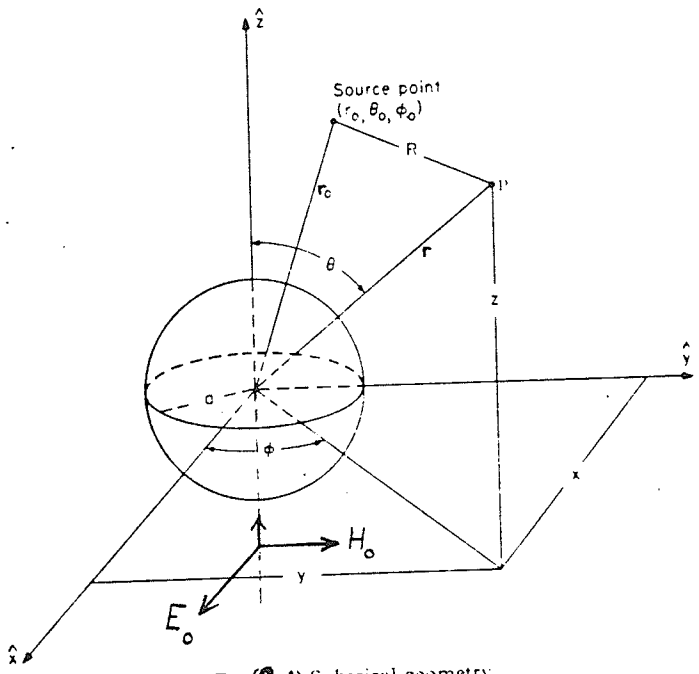

Fig.(2-1) Spherical geometry.

surface of the sphere is at $r = a$ and the spherical polar coordinates are related to the rectangular cartesian coordinates by the transformation

$$\begin{aligned} x &= r \sin\theta \cos\phi \ , \\ y &= r \sin\theta \sin\phi \ , \\ z &= r \cos\theta \end{aligned} \tag{2.1}$$

where $0 \leq r < \infty$, $0 \leq \theta \leq \pi$ and $0 \leq \phi \leq 2\pi$

2.2.2 Formulation

For a plane wave incident from the direction of the negative z-axis, the incident plane wave is defined by

$$\begin{aligned} E^i &= \hat{x}\, E_o \exp(-iKz) = \hat{x}\, E_o \exp(-iKr\cos\theta) \\ H^i &= \hat{y}\, \frac{E_o}{Z_o} \exp(-iKz) = \hat{y}\, \frac{E_o}{Z_o} \exp(-iKr\cos\theta) \end{aligned} \tag{2.2}$$

for a time factor $\exp(i\omega t)$ and where $Z_o = 120\pi$.
For convenience in applying boundary conditions, we must first expand the incident field in terms of spherical harmonics. This can be achieved by utilizing the relationship [8]

$$\exp(-iKr\cos\theta) = \sum_{n=0}^{\infty} (-i)^n (2n+1)\, P_n(\cos\theta)\, j_n(Kr) \tag{2.3}$$

where $P_n(\cos\theta)$ is the Legendre polynomial, and $j_n(Kr)$ is a spherical Bessel function, which is related to a cylindrical Bessel function $J_{n+\frac{1}{2}}(Kr)$ by

$$j_n(Kr) = \sqrt{\frac{\pi}{2Kr}}\ J_{n+\frac{1}{2}}(Kr) \tag{2.4}$$

The radial component of E^i is

$$E_r^i = \cos\phi \sin\theta\ E_x^i$$

$$= -\frac{iE_o \cos\phi}{(Kr)^2} \sum_{n=1}^{\infty} i^{-n}(2n+1)\ \hat{J}_n(Kr)\ P_n^1(\cos\theta) \tag{2.5}$$

where

$P_n^1(\cos\theta) = \frac{d}{d\theta} P_n(\cos\theta)$ is the associated Legendre polynomial,

$\hat{J}_n(Kr) = (Kr)\ j_n(Kr)$ is a spherical Riccati-Bessel function.

(Note that the $n = 0$ term of the summation drops out since $P_o^1(\cos\theta) = 0$.)

The total field components may be written in terms of potential functions A_r (TM) and F_r (TE) . The electromagnetic field in terms of A (magnetic vector potential) and F (electric vector potential) in free space is given by

$$E = -\nabla \times F + \frac{1}{i\omega\varepsilon_o} \nabla \times \nabla \times A$$

$$H = \nabla \times A + \frac{1}{i\omega\mu_o} \nabla \times \nabla \times F \tag{2.6}$$

Letting $A = A_r \hat{u}_r$, and $F = F_r \hat{u}_r$ and expanding equation (2.6), which is explicity

$$
\begin{aligned}
E_r &= \frac{1}{i\omega\varepsilon_o}\left(\frac{\partial^2}{\partial r^2} + K^2\right) A_r \\
E_\theta &= \frac{-1}{r\sin\theta}\frac{\partial F_r}{\partial\phi} + \frac{1}{i\omega\varepsilon_o r}\frac{\partial^2 A_r}{\partial r\partial\theta} \\
E_\phi &= \frac{1}{r}\frac{\partial F_r}{\partial\theta} + \frac{1}{i\omega\varepsilon_o \sin\theta}\frac{\partial^2 A_r}{\partial r\,\partial\theta} \\
H_r &= \frac{1}{i\omega\mu_o}\left(\frac{\partial^2}{\partial r^2} + K^2\right) F_r \\
H_\theta &= \frac{1}{r\sin\theta}\frac{\partial A_r}{\partial\theta} + \frac{1}{i\omega\mu_o r}\frac{\partial^2 F_r}{\partial r\partial\theta} \\
H_\phi &= \frac{-1}{r}\frac{\partial A_r}{\partial\theta} + \frac{1}{i\omega\mu_o \sin\theta}\frac{\partial^2 F_r}{\partial r\partial\theta}
\end{aligned}
\tag{2.7}
$$

The potential function A_r^i which gives rise to E_r^i, is easily found to be [8]

$$
A_r^i = + \frac{E_o \cos\phi}{\omega\mu_o} \sum_{n=1}^{\infty} a_n \hat{J}_n(Kr)\, P_n^1(\cos\theta) \tag{2.8}
$$

where

$$
a_n = \frac{i^{-n}(2n+1)}{n(n+1)}
$$

By similar procedure, it is found that

$$
F_r^i = + \frac{E_o \sin\phi}{K} \sum_{n=1}^{\infty} a_n \hat{J}_n(Kr)\, P_n^1(\cos\theta) \tag{2.9}
$$

To determine the field components outside the sphere, we again make use of A_r and F_r. These potentials consist of two parts: one part is contributed by the incident field (and which is given by

equations 2.8 and 2.9) and the other part is contributed by the scattered fields. It is possible to write

$$\begin{aligned} A_r &= A_r^i + A_r^s \\ F_r &= F_r^i + F_r^s \end{aligned} \tag{2.10}$$

Clearly, scattered potentials A_r^s and F_r^s have the same form as the incident potentials with $\hat{J}_n(Kr)$ replaced by the spherical Riccati-Hankel functions $\hat{H}_n^{(2)}(Kr)$. Thus, for the region $r > a$,

$$\begin{aligned} A_r &= + \frac{E_o \cos\phi}{\omega\mu_o} \sum_{n=1}^{\infty} (a_n \hat{J}_n(Kr) + b_n \hat{H}_n^{(2)}(Kr)) P_n^1(\cos\theta) \\ F_r &= + \frac{E_o \sin\phi}{K} \sum_{n=1}^{\infty} (a_n \hat{J}_n(Kr) + c_n \hat{H}_n^{(2)}(Kr)) P_n^1(\cos\theta) \end{aligned} \tag{2.11}$$

where b_n and c_n are coefficients unknown as yet and to be determined by an application of the boundary conditions on the surface of the sphere.

For a good conducting medium (most metal falls in this category), the field will penetrate an effective distance equal to the skin depth δ, which is given by [8]

$$\delta = \sqrt{\frac{2}{\omega\mu\sigma}} \tag{2.12}$$

When the radius of curvature is much larger than the skin depth, the boundary of the imperfect conductor may be described by an impedance boundary condition (occasionally called a Leontovich boundary condition in the literature). That is, the total fields E and H at the sur-

face are related by

$$E - (\hat{n}\cdot E)\hat{n} = Z(\hat{n}\cdot H) \tag{2.13}$$

where Z is the surface impedance and $\hat{n}$ is a unit vector normal to the surface.

It is now convenient to use the concept of the surface impedance boundary condition to determine the coefficients b_n and C_n in equation 2.1 . This requires that the total tangential components of E and H at $r = a$ be related as follows

$$\begin{aligned} E_\theta &= - Z H_\phi \\ E_\phi &= Z H_\theta \end{aligned} \tag{2.14}$$

The surface impedance Z is given by

$$Z = \sqrt{\frac{i\omega\mu}{i\omega\varepsilon + \sigma}} \tag{2.15}$$

For a highly conducting impedance sphere, Z can be given by

$$Z \simeq \sqrt{\frac{i\omega\mu}{\sigma}} = \frac{1 + i}{\sigma\,\delta} \tag{2.16}$$

with the displacement current being neglected by comparison with the conduction current. Using equations 2.7, 2.11 and 2.14 , we obtain [4]

$$\begin{aligned} b_n &= \frac{i^{-n}(2n + 1)}{n(n + 1)} B_n \\ c_n &= \frac{i^{-n}(2n + 1)}{n(n + 1)} C_n \end{aligned} \tag{2.17}$$

where

$$B_n = -\frac{\hat{J}_n'(Ka) - i\Delta\hat{J}_n(Ka)}{\hat{H}_n^{(2)'}(Ka) - i\Delta\hat{H}_n^{(2)}(Ka)}$$
$$C_n = -\frac{\Delta\hat{J}_n'(Ka) - i\hat{J}_n(Ka)}{\hat{H}_n^{(2)'}(Ka) - i\hat{H}_n^{(2)}(Ka)} \qquad (2.18)$$

with $\Delta = Z/Z_o$ being the normalized surface impedance. The prime denotes differentiation with respect to the argument.

It is particularly interesting to evaluate the scattered fields in the radiation region. This can be done by introducing the asymptotic value [9]

$$\hat{H}_n^{(2)}(Kr) \to i^{n+1} \exp(-iKr) \quad \text{as} \quad r \to \infty$$

It is now a simple matter to show that

$$E_\theta^s = \frac{-iE_o}{Kr} \exp(-iKr) \cos\phi\, P(\theta)$$
$$E_\phi^s = \frac{+iE_o}{Kr} \exp(-iKr) \sin\phi\, Q(\theta) \qquad (2.19)$$

where

$$P(\theta) = \sum_{n=1}^{\infty} \frac{(2n+1)}{n(n+1)} \left[B_n \frac{d}{d\theta} P_n^1(\cos\theta) + C_n \frac{P_n^1(\cos\theta)}{\sin\theta}\right]$$
$$Q(\theta) = \sum_{n=1}^{\infty} \frac{(2n+1)}{n(n+1)} \left[B_n \frac{P_n(\cos\theta)}{\sin\theta} + C_n \frac{d}{d\theta} P_n^1(\cos\theta)\right] \qquad (2.20)$$

The IBC method normally provides a solution with a relatively good accuracy [4] . Just how accurate the results are, is discussed below: Using the standard boundary value approach (not using IBC) the far-scattered field from a Lossy dielectric sphere characterized by ε_d , μ_d and σ has been shown to be of the form [8]

$$E^s_\theta = \frac{-i\, E_o}{Kr} \exp(-iKr)\cos\phi\; U(\theta)$$
$$E^s_\phi = \frac{i\, E_o}{Kr} \exp(-Kr)\sin\phi\; V(\theta) \qquad (2.21)$$

where

$$U(\theta) = \sum_{n=1}^{\infty} \frac{(2n+1)}{n(n+1)} \left(D_n \frac{d}{d\theta} P_n^1(\cos\theta) + E_n \frac{P_n^1(\cos\theta)}{\sin\theta}\right)$$
$$V(\theta) = \sum_{n=1}^{\infty} \frac{(2n+1)}{n(n+1)} \left(D_n \frac{P_n^1(\cos\theta)}{\sin\theta} + E_n \frac{d}{d\theta} P_n^1(\cos\theta)\right) \qquad (2.22)$$

and

$$D_n = -\frac{\hat{J}_n'(K_o a)\,\hat{J}_n(K_d a) - \Delta'\,\hat{J}_n(K_o a)\,\hat{J}_n'(K_d a)}{\hat{H}_n^{(2)'}(K_o a)\,\hat{J}_n(K_d a) - \Delta'\,\hat{H}_n^{(2)}(K_o a)\,\hat{J}_n'(K_d a)}$$
$$E_n = -\frac{\Delta'\,\hat{J}_n'(K_o a)\,\hat{J}_n(K_d a) - \hat{J}_n(K_o a)\,\hat{J}_n'(K_d a)}{\Delta'\,\hat{H}_n^{(2)'}(K_o a)\,\hat{J}_n(K_d a) - \hat{H}_n^{(2)}(K_o a)\,\hat{J}_n'(K_d a)} \qquad (2.23)$$

with

$$\Delta' = \sqrt{\frac{\varepsilon_o\,\mu_d}{\varepsilon_d\,\mu_o}}$$

In this case to include the skin depth effect, consider a sphere with $\sigma = 10^7$ mhos/m , a = 10 cm., $\mu_d = 20\,\mu_o$ and $\varepsilon_d = 4\,\varepsilon_o$. At a frequency of 1000 Hz, the quantity $i\omega\varepsilon_d + \sigma = i\omega\left(\varepsilon_d + \frac{\sigma}{i\omega}\right)$ provides an effective permittivity of

$$\hat{\varepsilon}_d = \frac{\sigma}{i\omega}$$

and a skin depth of

$$\delta = \sqrt{\frac{2}{\omega\mu_d\sigma}} = 1.125 \text{ mm.}$$

The argument of the spherical Bessel and Hankel functions $K_d a$ is complex and has the value

$$K_d a = 2\pi(1-i)\sqrt{200}$$

Figures 2.2 and 2.3 show the comparison of the scattered field from a Lossy dielectric sphere by using equation (2.21) and by using IBC method The close agreement between the two solutions is clearly evident.

2.3 Low Frequency Scattering by an Impedance Sphere

Let us now consider the far field scattered by a small impedance sphere. Assume an excitation frequency of 500 Hz and a sphere radius of 10 cm. (for which an experimental data in the time domain is available). Using small-argument approximation for the spherical Riccati-Bessel functions as $x \to 0$ one obtains [9]

$$\hat{J}_n(x) \to \frac{x^{n+1}}{1 \quad 3 \quad 5 \quad \ldots \quad (2n+1)}$$

$$\hat{Y}_n(x) \to -\frac{1 \quad 3 \quad 5 \quad \ldots \quad (2n-1)}{x^n} \qquad (2.24)$$

The far-scattered field can be obtained by using only the first term of equations (2.19). Considering only E_θ^s, the scattering function $P(\theta)$

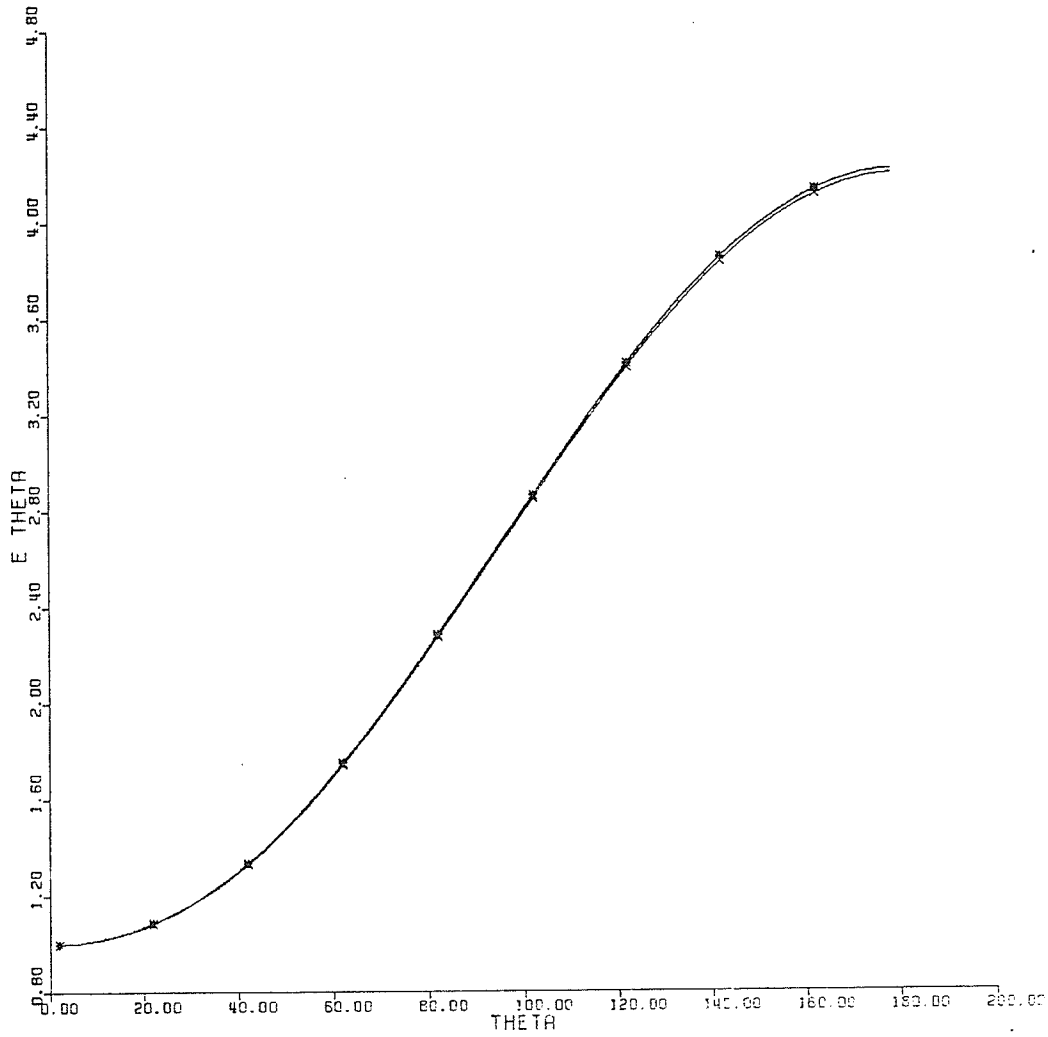

Fig. 2-2 Amplitude of E_θ. Comparison between the results based on Equ. 2-21 (*) and that based on IBC (x).

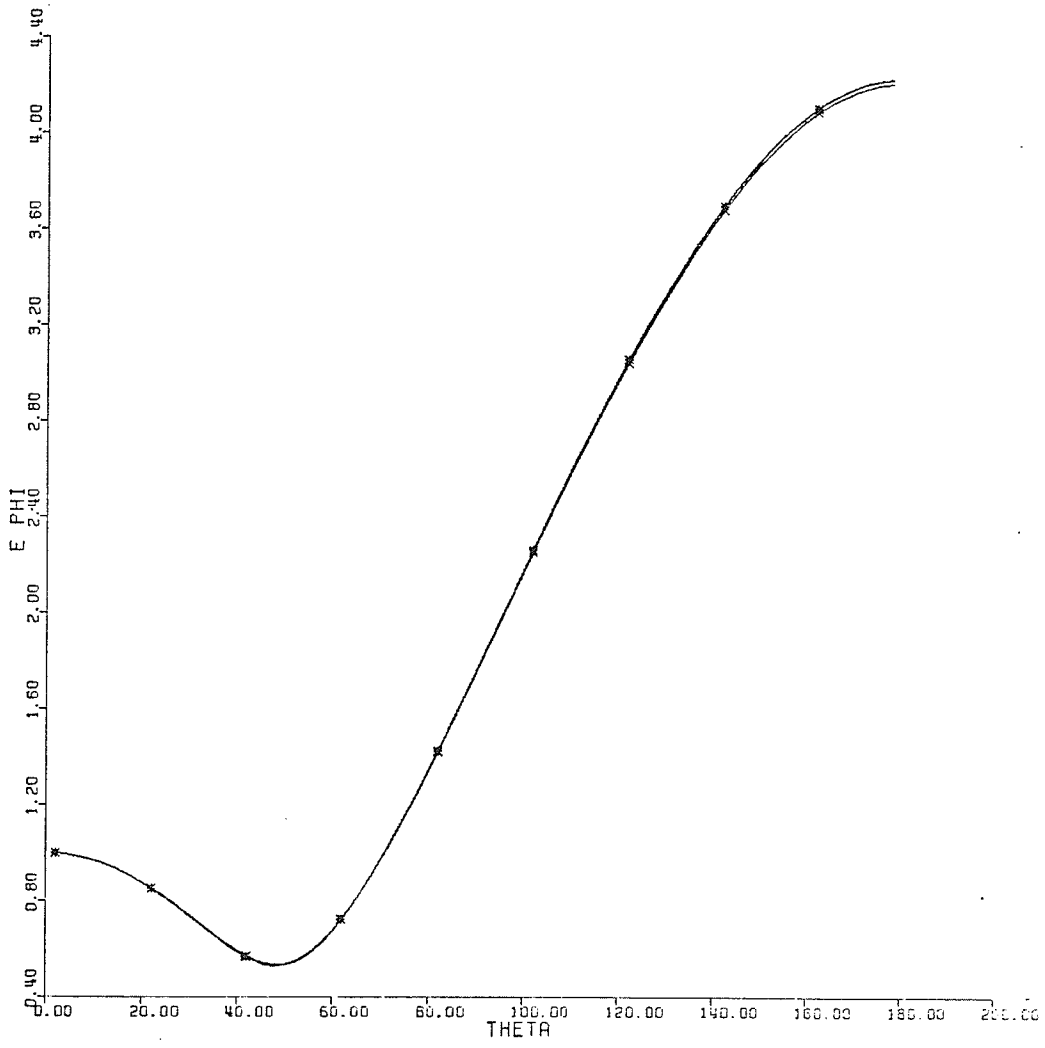

Fig. 2-3 Amplitude of E_{ϕ}. Comparison between the results based on Equ. 2-21 (*) and that based on IBC (x).

becomes (Appendix A)

$$P(\theta) = -1.5\ (B_1 \cos\theta + C_1) \tag{2.25}$$

where

$$B_1 = \frac{-2}{3}\ (Ka)^3 i$$

$$C_1 = \frac{-2}{3}\ (Ka)^2 (1.5A - 0.5(Ka)i)$$

and

$$A = \sqrt{\frac{\omega\mu}{2\sigma}}\ /Z_o$$

The numerical results for the scattering function $P(\theta)$ are plotted as a function of θ. The basic parameters are Ka and A.

Fig. 2.4 shows $P(\theta)$ for different values of A between 0 and 10^{-6} when $Ka = 10^{-6}$. It is evident from the curves in Fig. 2.4 that the back-scattering is much larger than the forward-scattering. Fig. 2.5 shows the back-scattered field as a function of (Ka) for values of A of 0 and 10^{-6}.

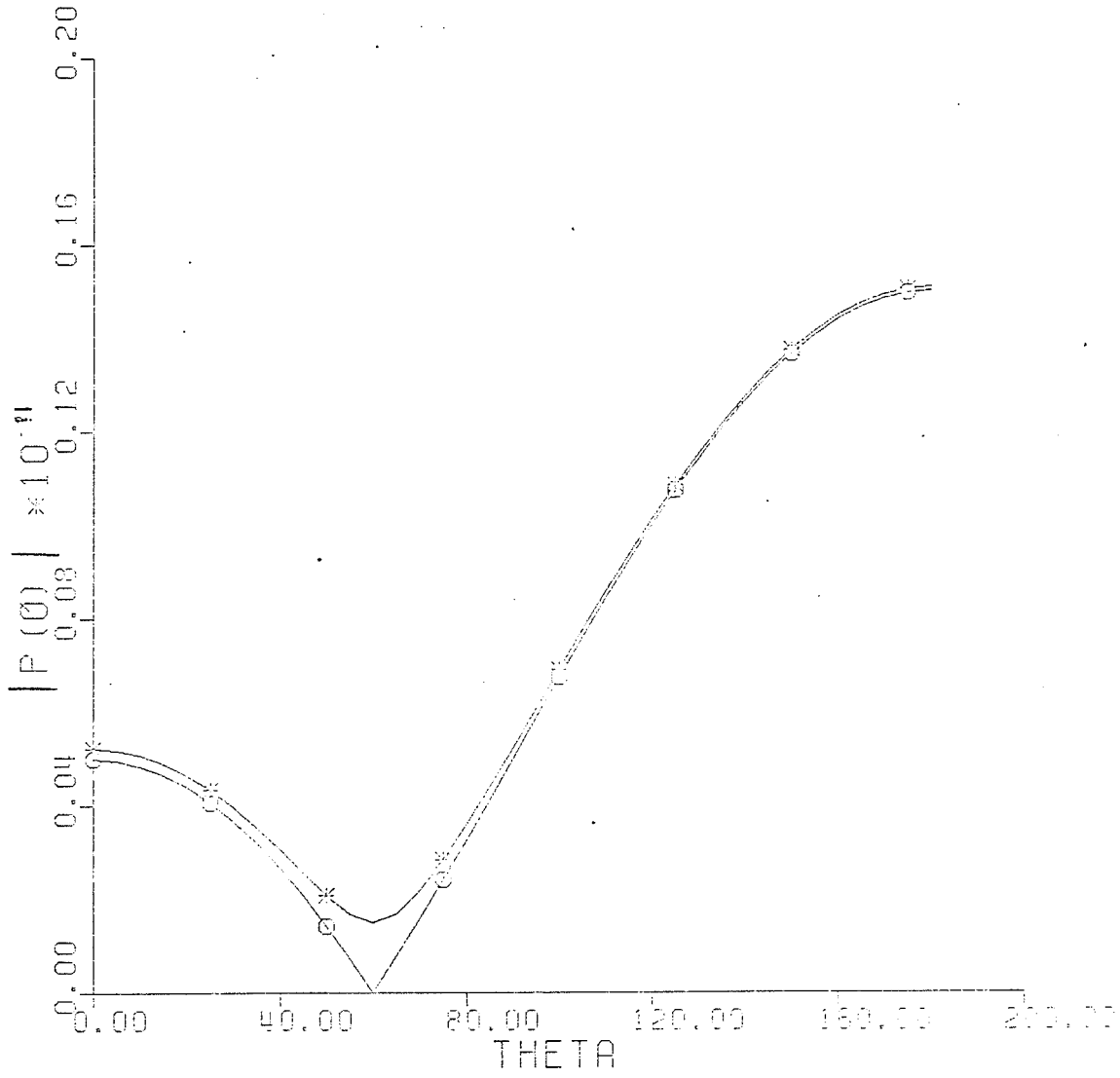

FIG. 2.4 Amplitude of the scattering function $P(\theta)$ as a function of scattering angle

* $A = 10^{-6}$ o $A = 0$

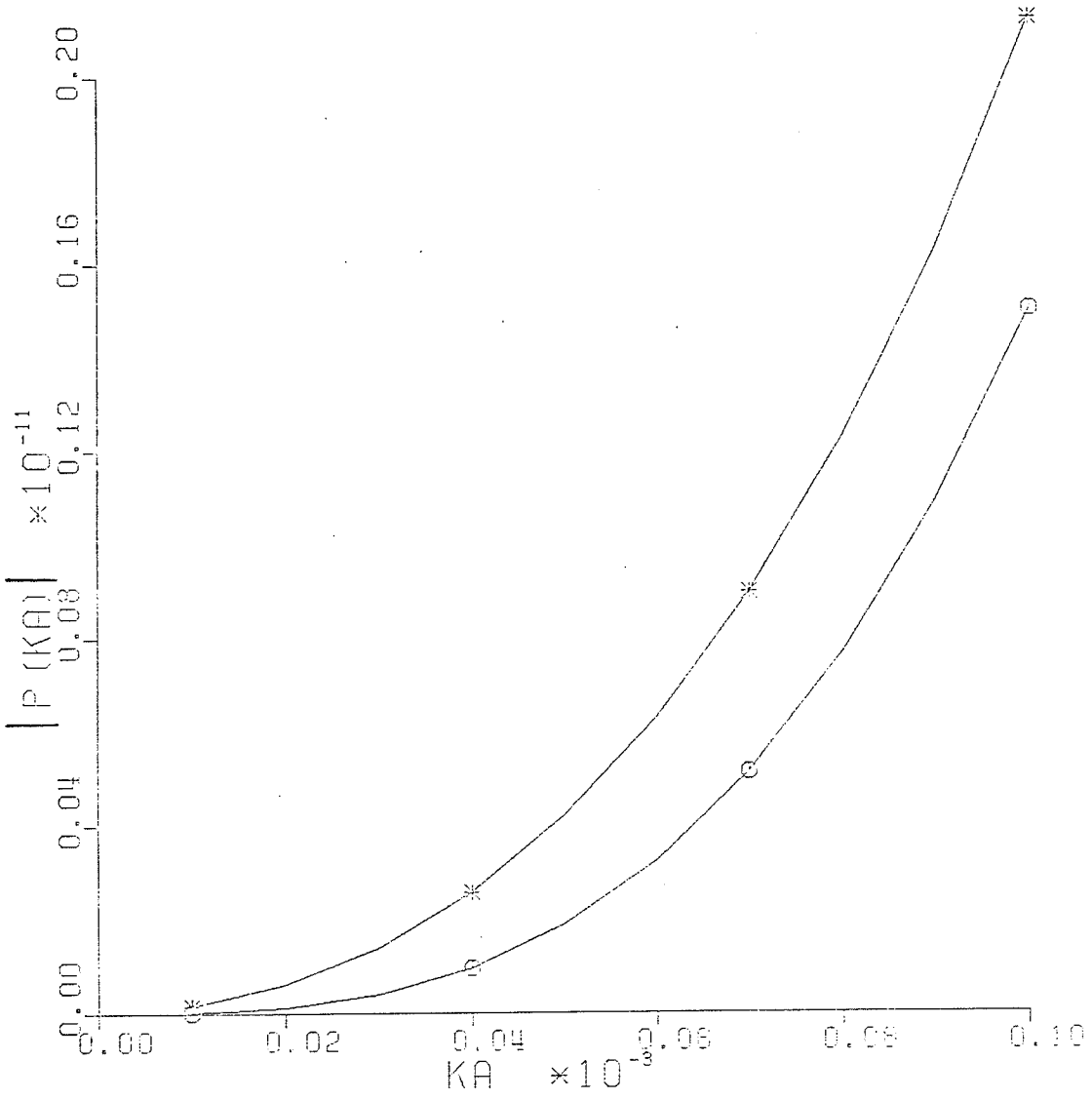

FIG. 2.5 Amplitude of the scattering function $P(\pi)$ as a function of (Ka)

* $A = 10^{-6}$ o $A = 0$

CHAPTER THREE

NEAR SCATTERED FIELD OF AN IMPEDANCE SPHERE EXCITED BY A UNIFORM CURRENT LOOP

3.1 Introduction

The radiation field of a radially directed electric dipole near a conducting sphere has been studied by Harrington [8]. In his analysis he has used the reciprocity theorem to obtain the solution. Fig. 3.2 shows a problem reciprocal to that of Fig. 3.1 in the sense that the component of E_1 in the direction of $I\ell_2$ equals the component of E_2 in the direction of $I\ell_1$. In the next sections we have solved the problem of near scattered field from an impedance sphere by the aid of the reciprocity theorem.

3.2 Excitation of a Sphere by a Uniform Current Loop

3.2.1 Formulation

The geometry of the problem is defined in terms of spherical coordinates (r,θ,ϕ) and the cartesian coordinates (x, y, z) with a common origin (O) and a common polar axis as shown in Fig. 3.3. Thus the surface of the sphere is at $r = a$, and is excited by a small current loop carrying a pulse train of fundamental frequency $f_o = 500Hz$.

To develop an analytical solution of the problem using impedance boundary conditions, a simplified geometry can be assumed in the following manner. Since the excitation loop is small at f_o we replace the exciting loop by a magnetic dipole at the centre of the transmitting loop. The direction of the assumed magnetic dipole is

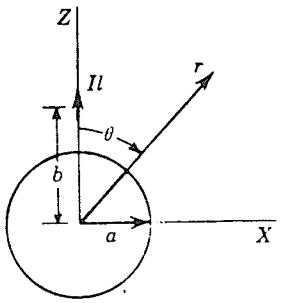

Fig. 3-1 An impedance sphere and a radially directed dipole.(Original problem)

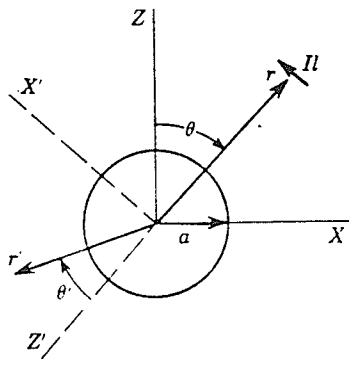

Fig. 3-2 Reciprocal problem.

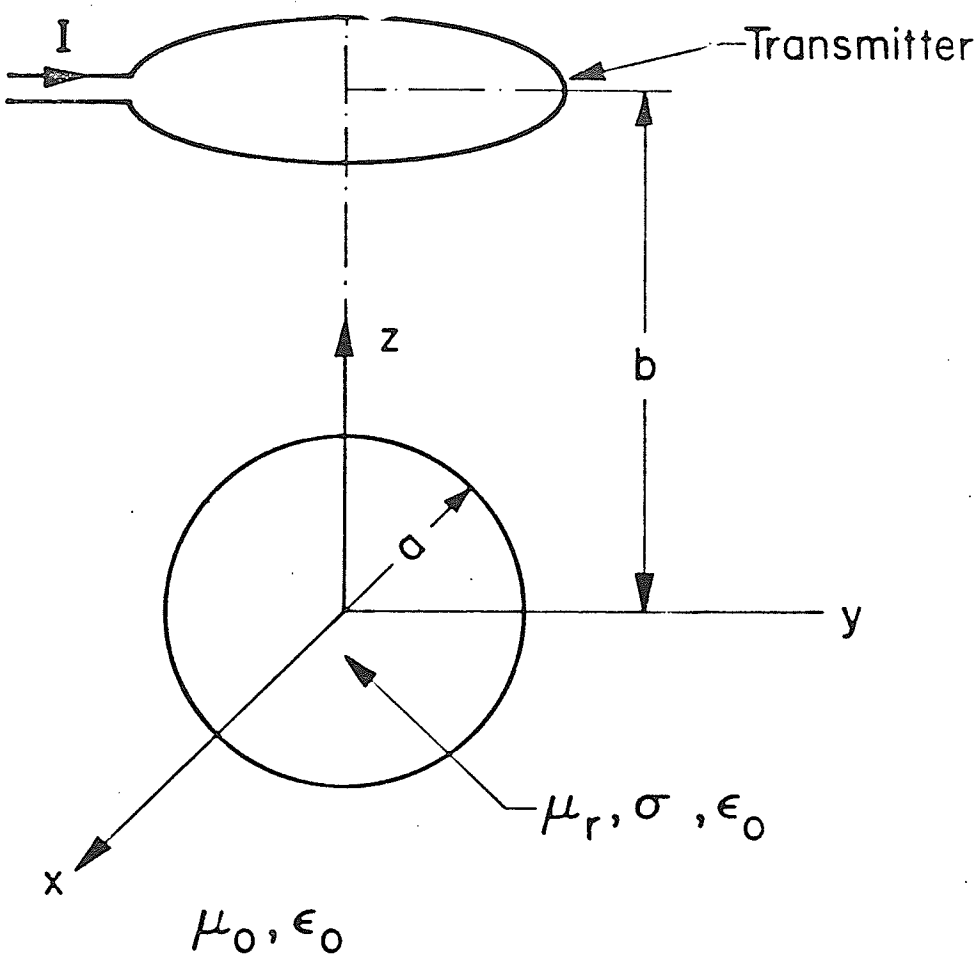

Fig. 3-3 Geometry of sphere excitation.

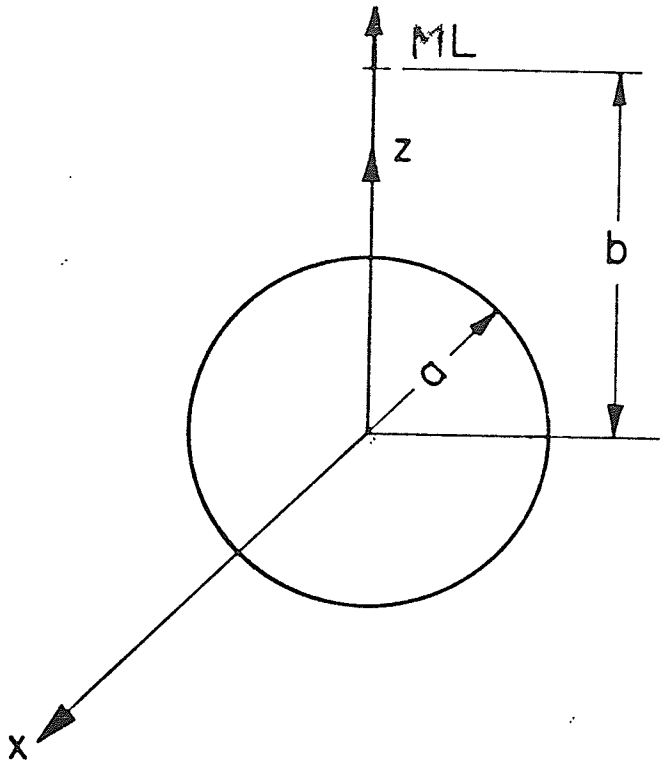

Fig. 3-4 Problem equivalent to Fig. 3-3

along the axis of the loop, Fig. 3.4. A solution for the scattered field using a magnetic dipole may be obtained by using the reciprocity relationship. This method is based on the following equivalence principle [18]: the reciprocity theorem states that the field received by a dipole located at far distances due to another dipole near the sphere is the same as the field of the far dipole received by the nearly dipole.

3.2.2 The Incident or Primary Fields

According to the equivalence principle, stated above we solved the scattering of a plane wave by a sphere and evaluated the scattered near field at a small distance 'b' near the sphere. This will give the far field of a dipole located at a distance 'b' from the origin of the sphere. Using this far scattered field, the vector potentials for the scattered field can be generated and utilized to compute the near field of a nearby dipole. Now, consider a plane wave travelling along z' - direction with the magnetic field polarized along the x' - direction, Fig. 3.4 . This wave has the form

$$H^i_{x'} = H_o \exp(-iKz') = H_o \exp(-iKr'\cos\theta') \tag{3.1}$$

The well-known theorem [5]

$$\exp(iKr\cos\theta) = \sum_{n=0}^{\infty} i^n(2n+1)\frac{\hat{J}_n(Kr)}{Kr} P_n(\cos\theta) \tag{3.2}$$

permits us to write

$$(H^i_{x'})^{\Pi} = H_o \sum_{n=0}^{\infty} i^n(2n+1) \frac{\hat{J}_n(Kr')}{Kr'} P_n(\cos\theta) \tag{3.3}$$

where H_o is the radiation field of a magnetic dipole $ML = SI$ (where S is the area of the loop and I is the current) and is given by

$$H_o = \frac{-i\ \omega\ \varepsilon_o\ (ML)}{4\pi r'} \exp(-iKr') \tag{3.4}$$

Therefore

$$(H^i_{r'})^{\Pi} = \cos\phi'\ \sin\theta'\ (H^i_{x'})$$

$$= \frac{H_o\ \cos\phi'}{iK^2\ r'^2} \sum_{n=1}^{\infty} i^{-n}(2n+1)\hat{J}_n(Kr')P^1_n(\cos\theta') \tag{3.5}$$

The potential function $F^i_{r'}$, which gives rise to $H^i_{r'}$ is easily found to be

$$F^i_{r'} = \frac{H_o}{\omega\varepsilon_o} \cos\phi' \sum_{n=1}^{\infty} a_n \hat{J}_n(Kr')P^1_n(\cos\theta') \tag{3.6}$$

where

$$a_n = \frac{i^{-n}(2n+1)}{n(n+1)} \tag{3.7}$$

By a similar procedure, it is found that

$$A^i_{r'} = \frac{H_o}{K} \sin\phi' \sum_{n=1}^{\infty} a_n \hat{J}_n(Kr')P^1_n(\cos\theta') \tag{3.8}$$

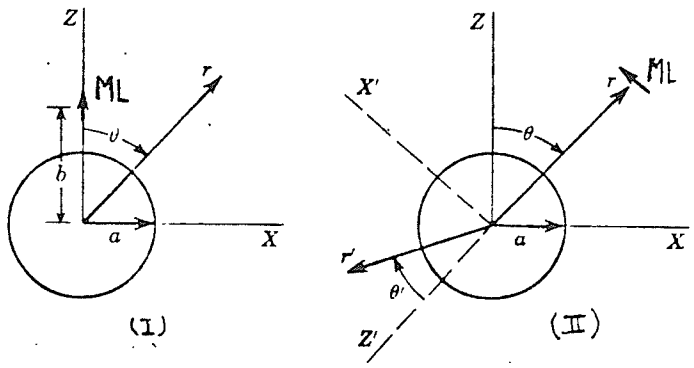

FIG. 3.5 An impedance sphere and a radially directed magnetic dipole. (I) original problem;
(II) reciprocal problem.

3.2.3 The Secondary or Scattered Field

For the region $r' > a$ it is possible to write

$$A_{r'} = A^i_{r'} + A^s_{r'}$$
$$F_{r'} = F^i_{r'} + F^s_{r'} \tag{3.9}$$

where the superscript s is associated with the scattered field. Clearly, $A^s_{r'}$ and $F^s_{r'}$ must contain the spherical Hankel functions $\hat{H}^{(2)}_n(Kr')$ in place of $\hat{J}_n(Kr')$ since the scattered field must behave as an outgoing wave at infinity. Thus for the region $r' > a$,

$$F^s_{r'} = \frac{H_o}{\omega\varepsilon_o}\cos\phi' \sum_{n=1}^{\infty} b_n \hat{H}^{(2)}_n(Kr')P^1_n(\cos\theta')$$
$$A^s_{r'} = \frac{H_o}{K}\sin\phi' \sum_{n=1}^{\infty} c_n \hat{H}^{(2)}_n(Kr')P^1_n(\cos\theta') \tag{3.10}$$

where b_n and c_n are unknown coefficients as yet to be determined.

The field components may be written in terms of potential functions A and F. Explicity,

$$E^{\Pi}_{\theta'} = \frac{-1}{r'\sin\theta'}\frac{\partial F_{r'}}{\partial\phi'},$$
$$H^{\Pi}_{\theta'} = \frac{1}{i\omega\mu_o r'}\frac{\partial^2 F_{r'}}{\partial r'\partial\theta'},$$
$$E^{\Pi}_{\phi'} = \frac{1}{r'}\frac{\partial F_{r'}}{\partial\theta'}, \tag{3.11}$$
$$H^{\Pi}_{\phi'} = \frac{1}{i\omega\mu_o r'\sin\theta'}\frac{\partial^2 F_{r'}}{\partial r'\partial\phi'},$$
$$H^{\Pi}_{r'} = \frac{1}{i\omega\mu_o}\left(\frac{\partial^2}{\partial r'^2} + K^2\right)F_{r'}$$

It is now convenient to use the surface impedance boundary conditions such that the relation between the tangential field components at $r = a$ are to be prescribed. Therefore on the surface of the sphere with a surface impedance Z the relationship

$$E^{II}_{\theta'} = - ZH^{II}_{\phi'} \tag{3.12}$$

gives

$$\frac{\partial F_{r'}}{\partial \phi'} = \frac{Z}{i\omega\mu_o} \frac{\partial^2 F_{r'}}{\partial r' \partial \phi'} \tag{3.13}$$

or

$$F_{r'} = \frac{Z'}{i\omega\mu_o} \frac{\partial F_{r'}}{\partial r'} \tag{3.14}$$

Therefore

$$\sum_{n=1}^{\infty} (a_n \hat{J}_n(Ka) + b_n \hat{H}^{(2)}_n(Ka)) P'_n(\cos\theta')$$

$$= \frac{ZK}{i\omega\mu_o} \sum_{n=1}^{\infty} (a_n \hat{J}'_n(Ka) + b_n \hat{H}^{(2)'}_n) P'_n(\cos\theta') \tag{3.15}$$

Because of the orthogonality of $P^m_n(\cos\theta)$, we get

$$b_n = - a_n \frac{\Delta \hat{J}'_n(Ka) - i \hat{J}_n(Ka)}{\Delta \hat{H}^{(2)'}_n(Ka) - i \hat{H}^{(2)}_n(Ka)} \tag{3.16}$$

where $\Delta = Z/Z_o$ is the normalized surface impedance.

Using the reciprocity theorem, $H^{II}_{r'}$ evaluated at $r' = b$, $\theta' = \pi - \theta$, $\phi' = 0$ must be equal to H^I_θ at (r, θ, ϕ). Thus using the relationship

$$P_n'(\cos(\pi-\theta)) = (-1)^n P_n'(\cos\theta) \tag{3.17}$$

and

$$H_{r'}^{II} = (H_{r'}^{i} + H_{r'}^{s})^{II}$$

$$= \frac{1}{i\omega\mu_o}\left(\frac{\partial^2}{\partial' r^2} + K^2\right)(F_{r'}^{i} + F_{r'}^{s}) \tag{3.18}$$

the far scattered field of the magnetic dipole located at (b, o, o) has the form

$$(H_\theta^s)^I = \frac{i\, H_o}{K^2 b^2} \sum_{n=1}^{\infty} (-1)^n n(n+1) b_n \hat{H}_n^{(2)}(Kb) P_n'(\cos\theta) \tag{3.19}$$

(Note that superscripts I, II refer to Fig. 3.5 I and II).

3.3 Near Scattered Field

To obtain the near scattered field the vector potential may be constructed as

$$F_r^s = \sum_{n=1}^{\infty} e_n \hat{H}_n^{(2)}(Kr) P_n(\cos\theta) \tag{3.20}$$

and then the far scattered magnetic field H_θ is

$$H_\theta^s = \frac{1}{i\omega\mu_o r} \frac{\partial^2 F_r^s}{\partial r \partial\theta} \tag{3.21}$$

The coefficients e_n can be obtained by a comparison of the expression given by equation (3.21) as $Kr \to \infty$ with the corresponding expression for H_θ^s given by equation (3.19). The distant scattered

field can be found from the general expression (3.21) by using the assymptotic formula [9]

$$\hat{H}_n^{(2)}(Kr) \to i^{n+1} \exp(-iKr) \tag{3.22}$$

Therefore equation (3.21) reduced to

$$\hat{H}_\theta^s = \frac{K}{i\omega\mu_o r} \exp(-iKr) \sum_{n=1}^{\infty} i^n e_n P_n^1(\cos\theta) \tag{3.23}$$

By equating this expression to (3.19) one gets

$$\frac{K}{i\omega\mu_o r} \exp(-iKr) \sum_{n=1}^{\infty} i^n P_n^1(\cos\theta) e_n$$

$$= \frac{i H_o}{K^2 b^2} \sum_{n=1}^{\infty} (-1)^n n(n+1) b_n \hat{H}_n^{(2)}(Kb) P_n^1(\cos\theta) \tag{3.24}$$

where H_o is given by (3.4) and b_n is given by (3.16). The result is

$$e_n = \frac{-i(ML)}{4\pi b^2 K} (2n+1)\left(\frac{-b_n}{a_n}\right)\hat{H}_n^{(2)}(Kb) \tag{3.25}$$

where a_n is given by (3.7).

Therefore for $r > b$, the near scattered field components can be obtained in the form

$$H^S = \frac{-(ML)}{4\pi b^2 \omega\mu_o r} \sum_{n=1}^{\infty} (2n+1)\left(\frac{-b_n}{a_n}\right)\hat{H}_n^{(2)}(Kb)$$

$$\cdot \hat{H}_n^{(2)}(Kr) P_n^1(\cos\theta) \tag{3.26}$$

$$E_{\phi}^{s} = \frac{+i(ML)}{4\pi b^2 Kr} \sum_{n=1}^{\infty} (2n+1)\left(\frac{-b_n}{a_n}\right)\hat{H}_n^{(2)}(Kb)$$

$$\cdot \hat{H}_n^{(2)}(Kr)\ P_n^1(\cos\theta) \qquad (3.27)$$

$$H_r^{s} = \frac{-(ML)}{4\pi b^2 \omega K \mu_o r^2} \sum_{n=1}^{\infty} n(n+1)(2n+1)\left(\frac{-b_n}{a_n}\right)$$

$$\cdot \hat{H}_n^{(2)}(Kb) \cdot \hat{H}_n^{(2)'}(Kr)\ P_n^1(\cos\theta) \qquad (3.28)$$

From a practical point of view, the near scattered field may be measured by a small receiving loop such that the axis of the loop lies along the z-direction and its location is just above the transmitter at a distance 'C' from the sphere centre. Now, the field induced in the receiving loop is due to H_z, which for small loops is approximately equal to H_r [18]. Therefore for determining the received signal, only H_r is required. To simplify the process, equation (3.28) could be rewritten in the form

$$H_r^{s} = \frac{-ML}{4\pi b^2 \omega \mu_o K r^2}\ Q(\theta) \qquad (3.29)$$

where

$$Q(\theta) = \sum_{n=1}^{\infty} n(n+1)(2n+1)\left(\frac{-b_n}{a_n}\right)$$

$$\cdot \hat{H}_n^{(2)}(Kb) \cdot \hat{H}_n^{(2)'}(Kr)\ P_n^1(\cos\theta) \qquad (3.30)$$

3.4 Low Frequency Approximations

When the incident field is a pulse train of 50% duty cycle and the excitation frequency, f_o = 500Hz as shown in Fig. 3.6, it can be represented by

$$H^i = \sum_{n=1}^{\infty} A_m(m\omega_o) \cos(m\omega_o t) \tag{3.31}$$

where

$$A_m = \begin{cases} 0 & m \text{ even} \\ \frac{2}{m} & m \text{ odd} \end{cases}$$

At this low excitation frequency f_o, the low frequency approximation can be used for a wide range of harmonics of the fundamental frequency f_o. At the above value of f_o and sphere radii in the range of 10 cm., the near scattered field which is given by equation (3.29) by using only the first term of the series, in terms of $x1 = Ka$, $x2 = Kb$, $x3 = Kc$ and $\Delta = z/z_o = A(1+i)$. Note that A is a function of (ω, μ, σ).

After the necessary manipulations (Appendix B) we find that (in the back scattered direction $\theta = \pi$)

$$Q = \frac{2 x_1^3}{x_2 x_3 (x_1 + 2A)} (3A + i(A - x1)) \tag{3.32}$$

where $x_1 = Ka$, $x_2 = Kb$, $x_3 = Kc$ and

$$A = \sqrt{\frac{\omega\mu}{\sigma}} / z_o$$

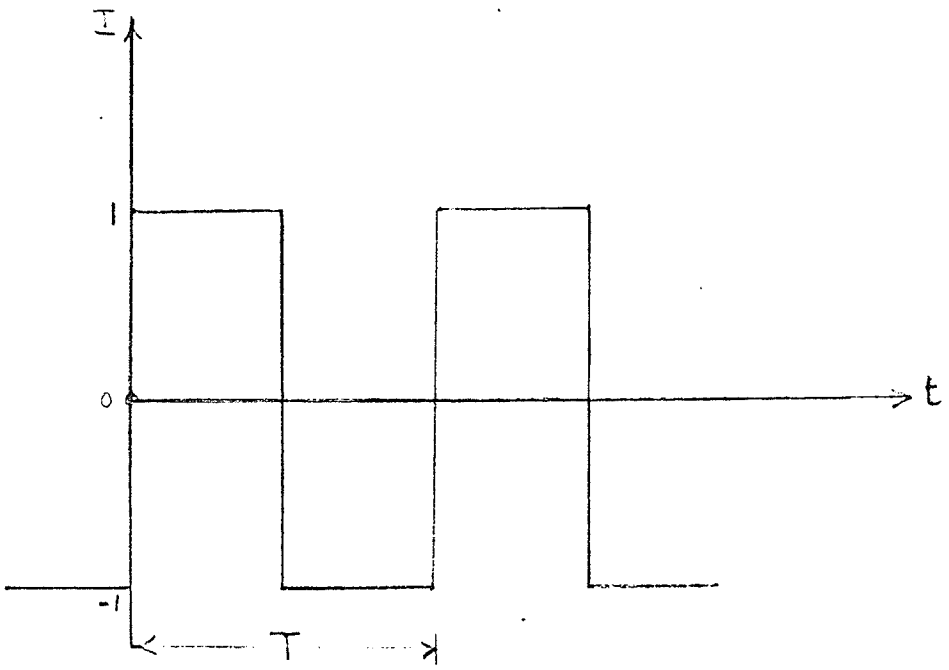

Fig. 3.6 Excitation waveform.

In Chapter Five the results are used to determine the sphere size and physical properties using scattered field.

CHAPTER FOUR

TRANSIENT SCATTERING BY USING IMPEDANCE BOUNDARY CONDITONS

4.1 Introduction

The scattering of plane electromagnetic waves by a sphere in the time domain has been considered by many investigators. The scattering of short electromagnetic pulses by a conducting sphere has been studied by Kennaugh [11]. The back-scattering of short plane-wave pulses by perfectly conducting spheres has been investigated for both near and far fields by Weston [12] by using an inverse Laplace transform. Wait and Hill [14] have shown that the more general problem of a spherical shell of arbitrary thickness can be treated by using an inverse Fourier transform.

It is the purpose of this chapter to explore the possibility of computing the transient response of a sphere with impedance boundary conditions using the frequency domain data. The interest is in the back scattering of the magnetic field due to a small current loop carrying a square wave of fundamental frequency f_o .

4.2 Formulation

The incident field again will be assumed due to a magnetic dipole, located axially at the centre of the transmitting coil. The incident wave is a pulse train with a 50% duty cycle at a frequency f_o . Therefore it can be represented by

$$H^i = \sum_{m=1}^{\infty} A_m \cos(m\omega_o t) \tag{4.1}$$

where

$$A_m = \begin{cases} 0 & m \text{ even} \\ \frac{2}{m\pi} & m \text{ odd} \end{cases} \tag{4.2}$$

To compute the time response of the scattered field, it is assumed that the sphere and space combination is a linear system, with the input signal H^i given by (4.1).

Considering each term of (4.1) the corresponding scattered near field can be computed using equation (3.29). Again we select H_r^s as an approximation to Hz , which is proportional to the induced current in the receiving coil. To obtain the time response the transfer function of the linear system made of space and the scatterer must be first obtained by normalizing the scattered field H_r^s by the incident field H_r^i . To compute the incident magnetic field, it is assumed that the observation point (receiver coil) is located just above the transmitter coil at a distance 'c' from the centre of sphere, Fig. 3.2 . The incident magnetic field can then be written as (Appendix C)

$$H_r^i(r) = \frac{(ML)}{2\pi i\omega\mu_o r^3} \left(\frac{-iK(r-b)-1}{(r-b)^2}\right) \exp(-iK(r-b)) \tag{4.3}$$

The transfer function of the system has the form H_r^s/H_r^i where H_r^i and H_r^s are given by (4.3) and (3.29) at $\theta = \pi$ and $r = c$ respectively. Utilizing the transfer function one can then show that the time response of the sphere is given by

$$F(t) = \mathrm{Re} \sum_{m=1}^{\infty} A_n f_n(in\omega_o) \exp(in\omega_o t) \tag{4.4}$$

where

$$f_n(in\omega_o) = \frac{H_r^s}{H_r^i} \tag{4.5}$$

and A_n is given by (4.2).

Figures 4.1 to 4.7 show that the time response $F(t)$ depends strongly on the location, size and the physical parameters of the sphere. It is evident that the time response behaviour depends on all parameters involved. However, to understand the behaviour of the response we will discuss its dependence on each parameter separately.

Figures 4.1 and 4.2 show the dependence of the response on the parameter 'c', the location of the receiving loop. The initial rate of decay is higher for small 'c', but the response for small 'c' after the initial decay remains relatively constant. On the other hand, the response for large 'c' continues decaying until the wave form changes. The opposite situation holds for the parameter 'b', the location of the transmitting loop. Fig. 4.3 shows that for large 'b' the response decays faster initially, but afterward tends to remain at a relatively constant level.

In Figures 4.4 to 4.6 the time response are shown for different values of sphere radius 'a' . These figures show that for small 'a' the response decays faster initially, but afterward remains relatively constant. In this regard, the dependence of the response on 'a' is similar to its dependence on 'c' .

Finally, Fig. 4.7 shows the dependence of the response on the permeability of the sphere. The rate of decay increases as the permeability increases.

By an examination of the experimental data supplied by DRES (Defence Research Establishment Suffield), where steel spheres were excited by square pulse trains of a fundamental frequency f_o = 500 Hz, it is found that the above calculated data agrees well with the experimental results.

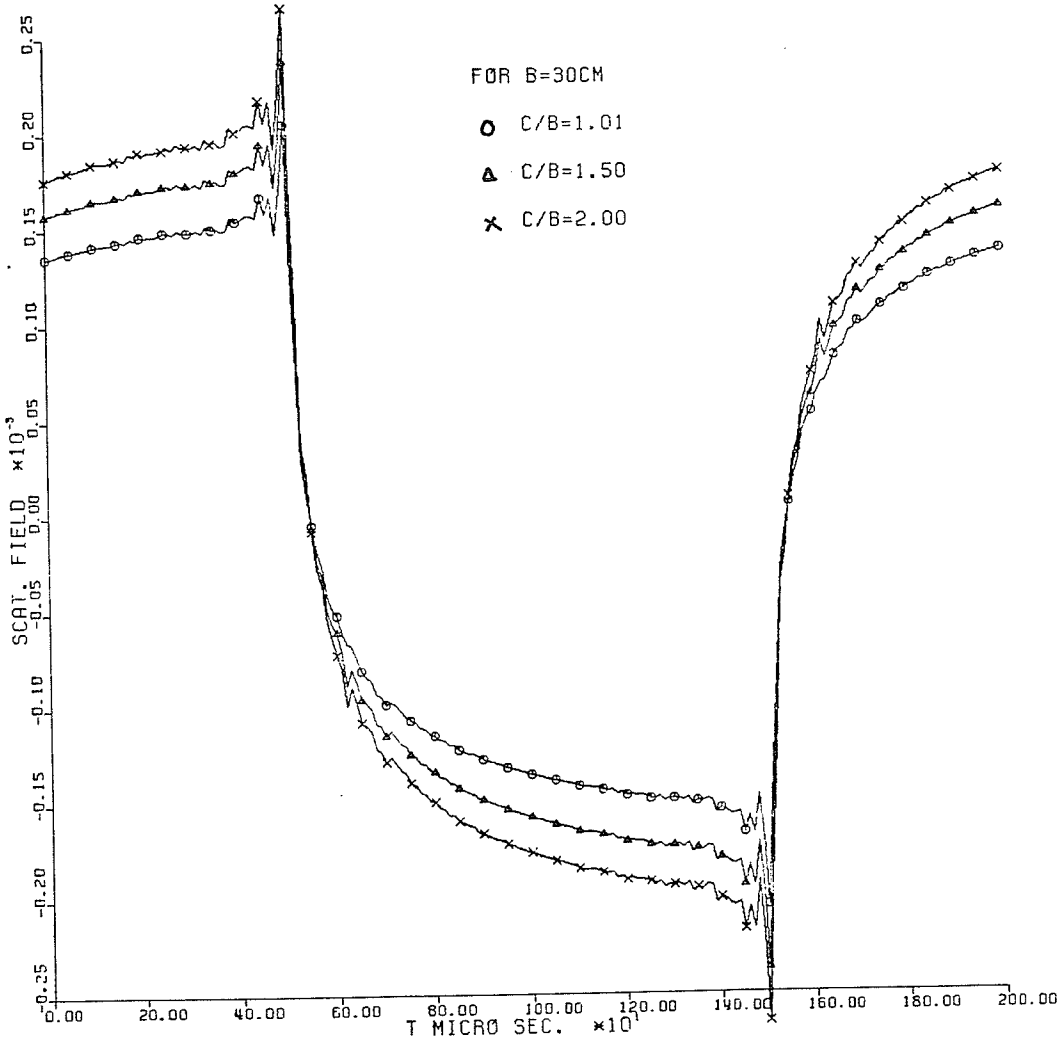

FIG. 4.1 Time response of a sphere for different c , a = 3.8 cm., μ_r = 500 .

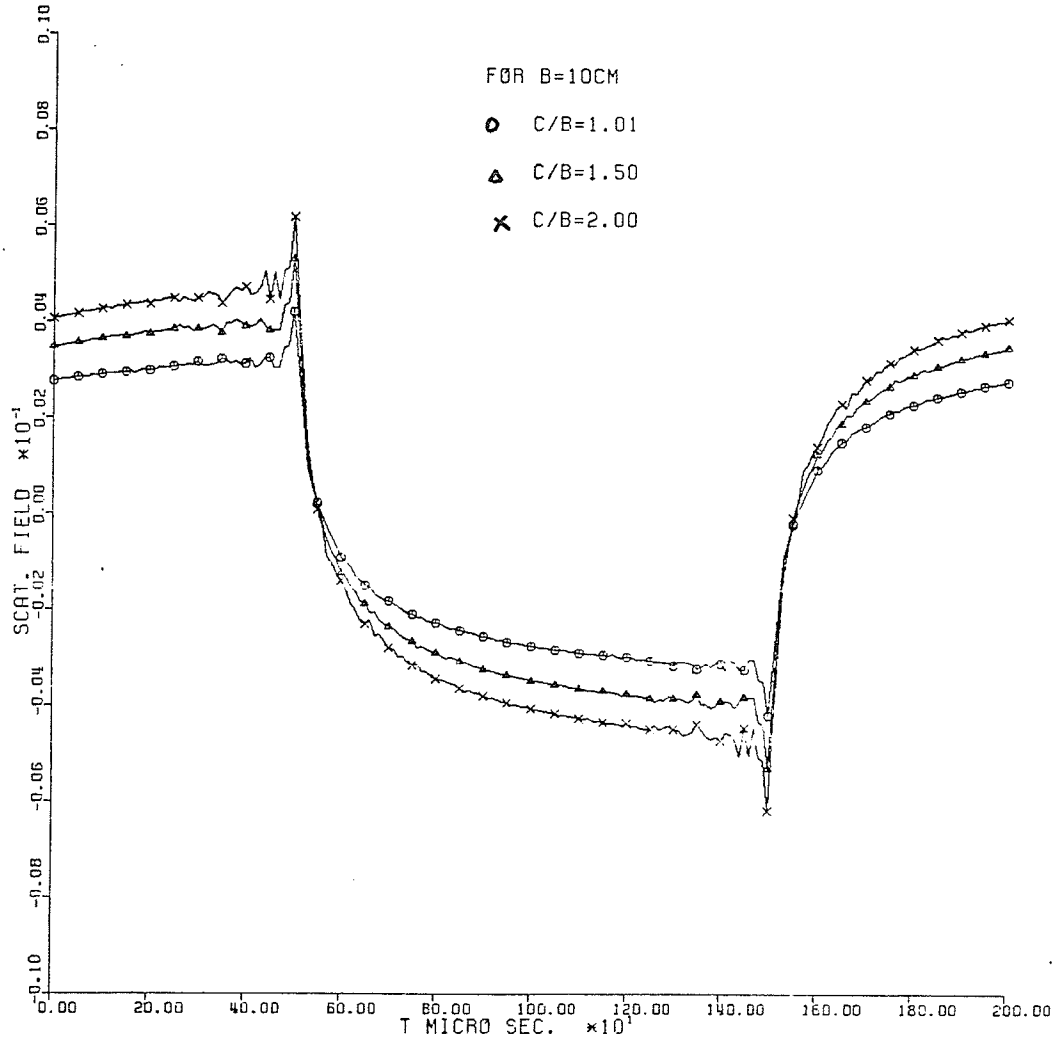

FIG. 4.2 Time response of a sphere for different c , a = 3.8 cm., μ_r = 500 .

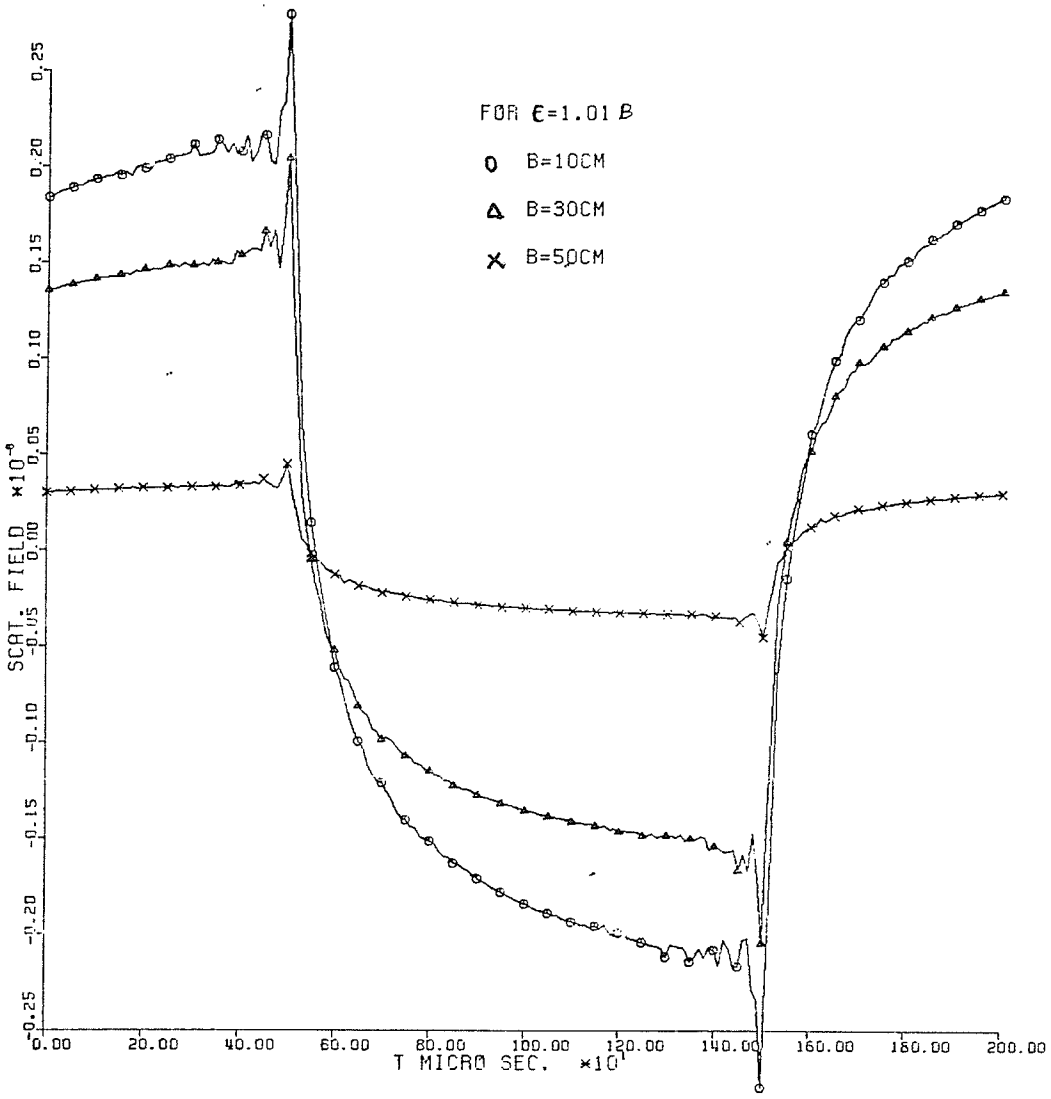

FIG. 4.3 Time response of a sphere for different b ,
a = 3.8 cm., μ_r = 500 .

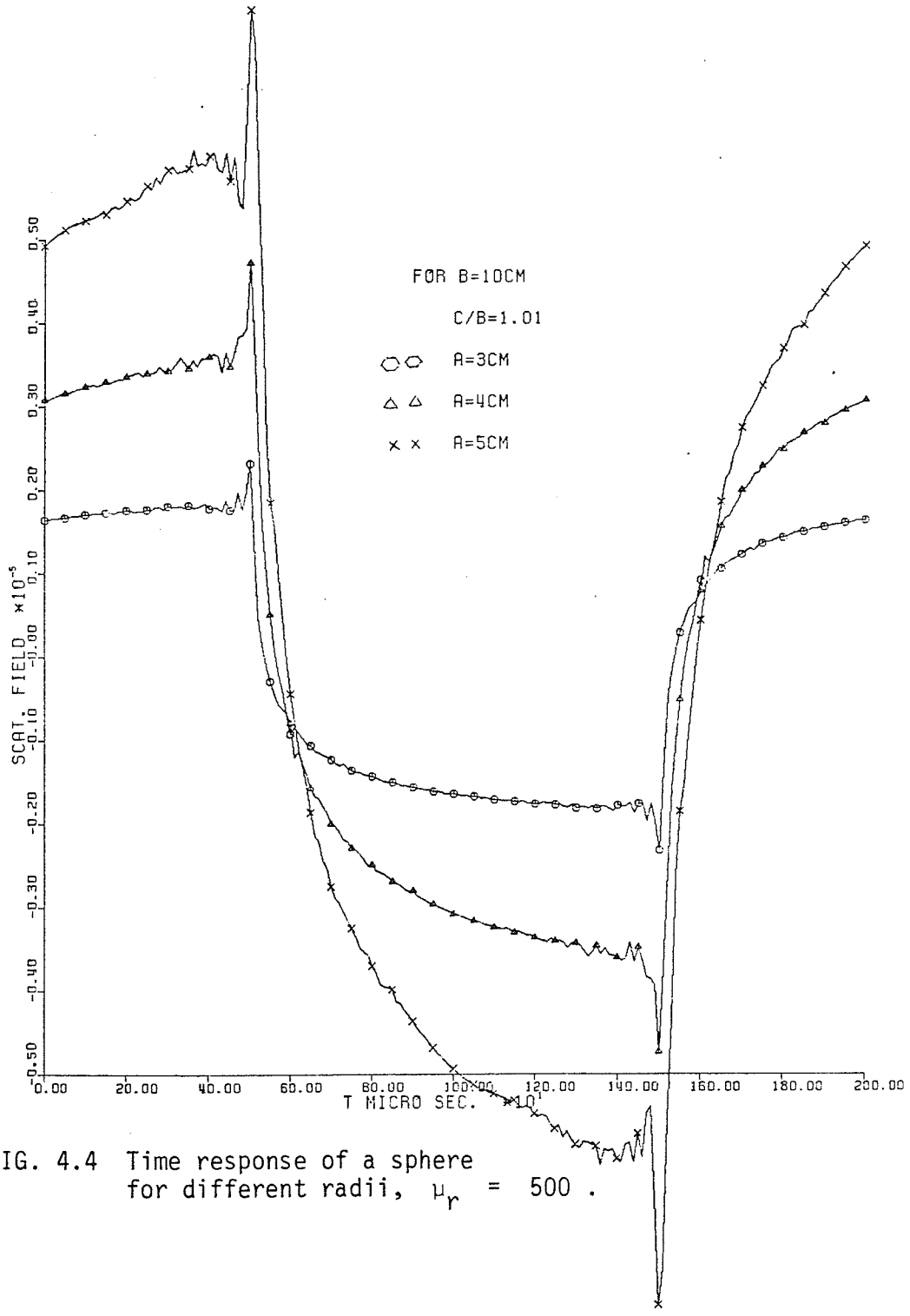

FIG. 4.4 Time response of a sphere for different radii, $\mu_r = 500$.

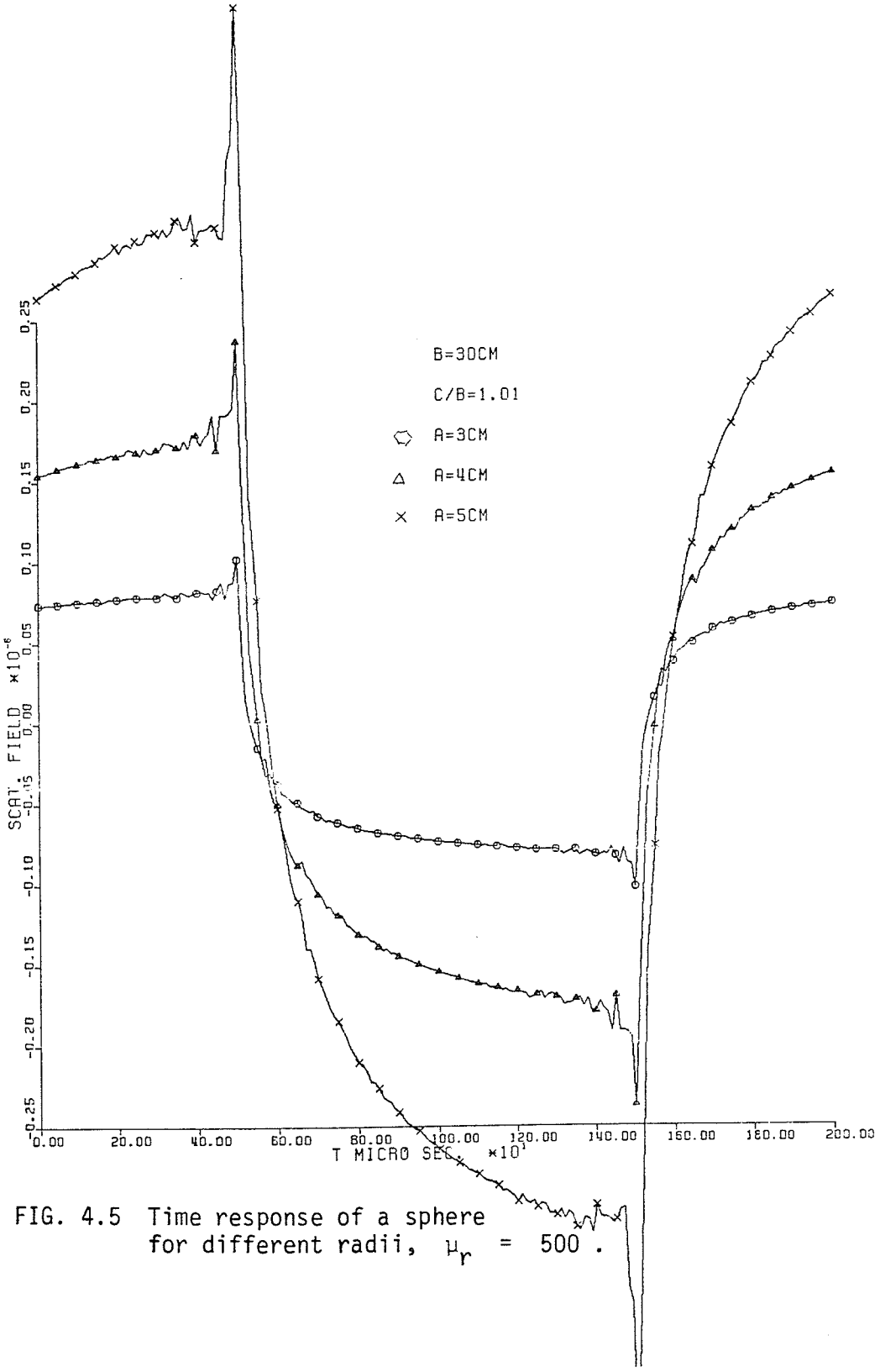

FIG. 4.5 Time response of a sphere for different radii, $\mu_r = 500$.

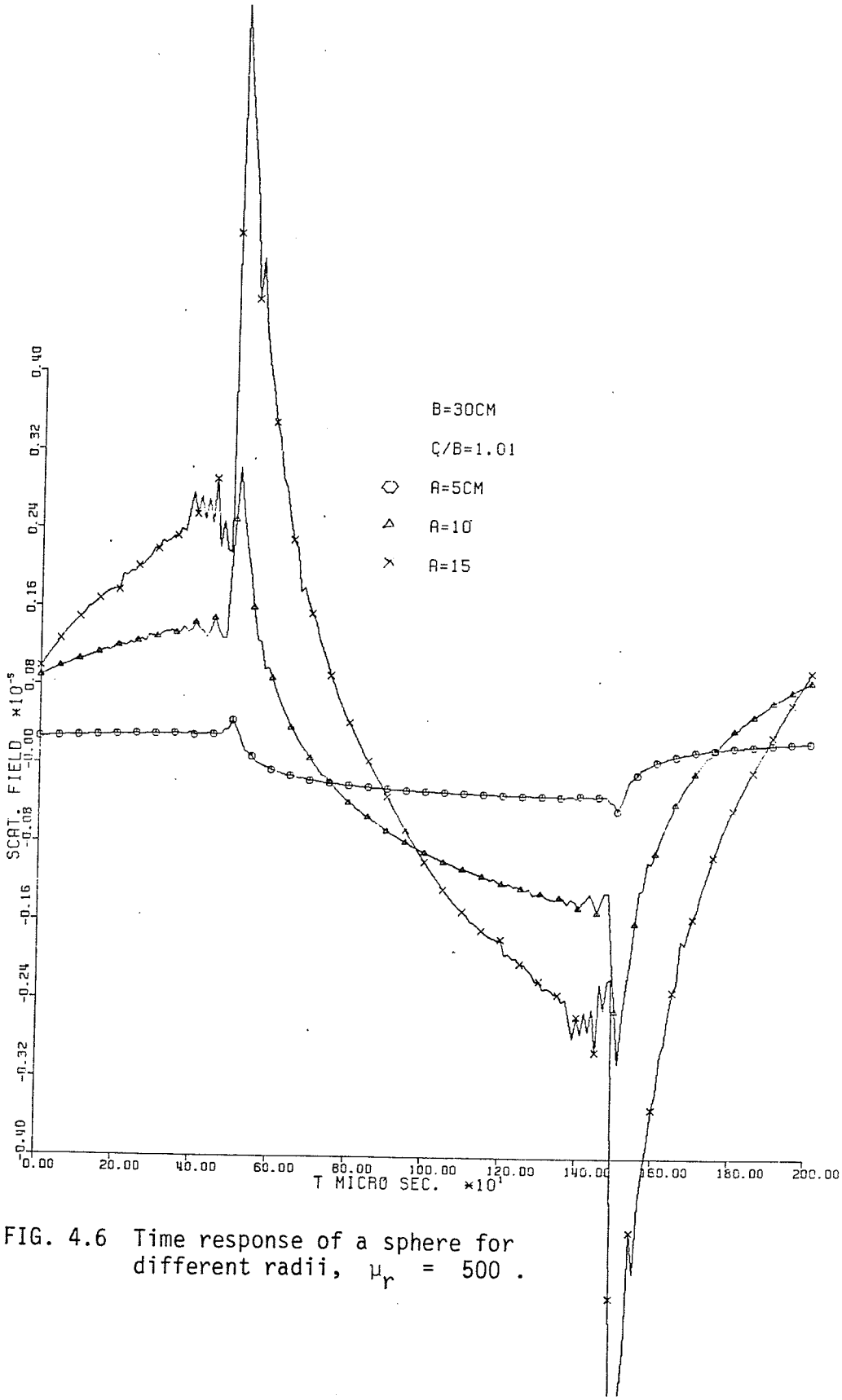

FIG. 4.6 Time response of a sphere for different radii, $\mu_r = 500$.

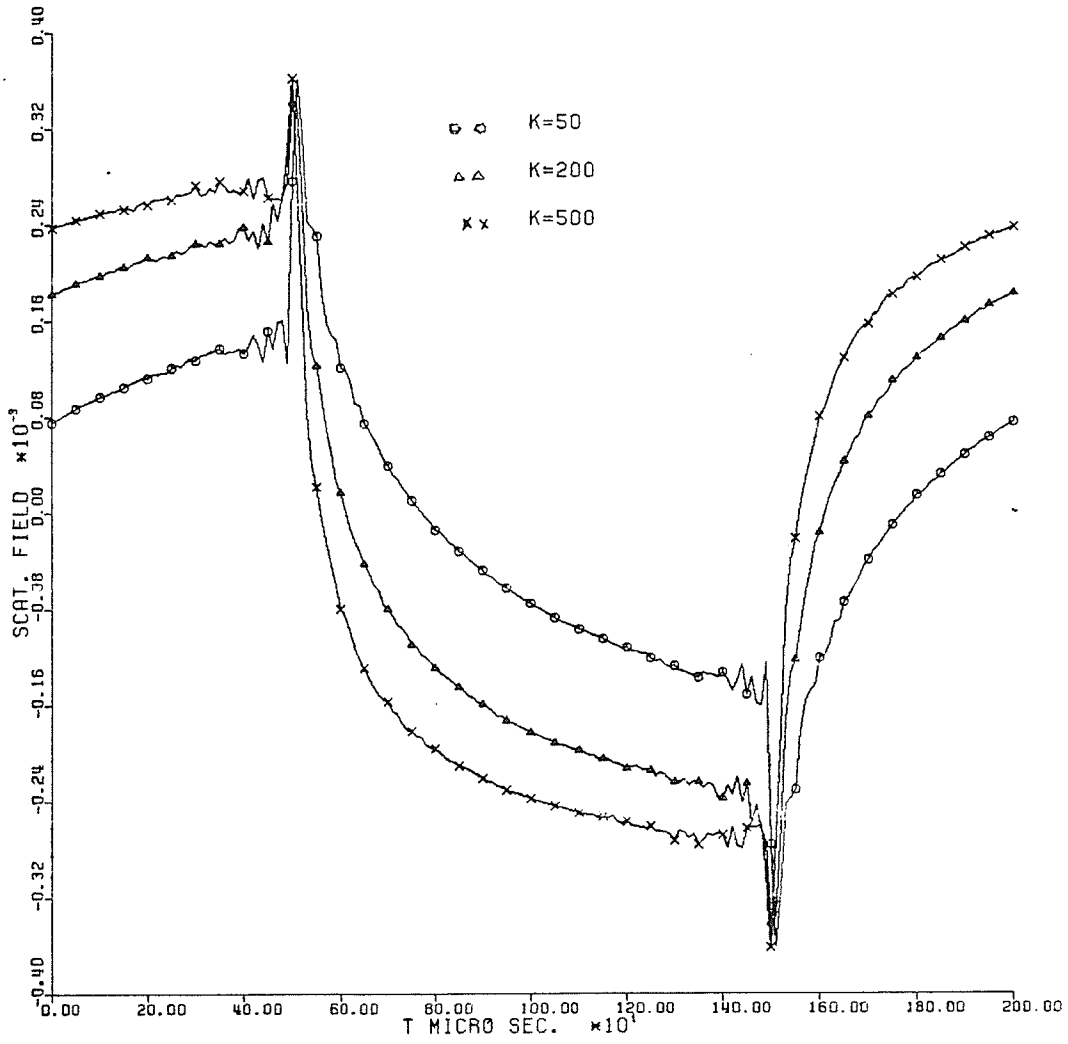

FIG. 4.7 Time response of a sphere for different permeability ($K = \mu_r$), b = 10 cm., c/b = 1.01, a = 3.8 cm.

CHAPTER FIVE

APPLICATION OF IBC FOR TARGET IDENTIFICATION

5.1 Introduction

In Chapters Two, Three and Four the study of the scattered field from an impedance sphere shows that a simple expression for the scattered field can be obtained either in the frequency domain or in the time domain. Using those simplified expressions, one can show that the scattered field may be used to determine the size and the electrical properties of a scattering sphere. In the following sections, we discuss the method of the determination of these parameters by using available data either in the frequency domain or in the time domain.

5.2.1 Plane Wave Incident

Consider an incident plane wave which has a pulse train wave form of 50% duty cycle and a fundamental frequency f_o . Such a field can be represented by

$$E^i = \sum_{n=1}^{\infty} A_n(n\omega_o) \cos(n\omega_o t) \qquad (5.1)$$

where

$$A_n = \begin{cases} 0 , & n \text{ even} \\ \frac{2}{n\pi} , & n \text{ odd} \end{cases}$$

At low frequency excitation (e.g. for small f_o), the low frequency approximation developed in Chapter Two can be used for a wide range of harmonics of the fundamental frequency f_o. For example, for $n = 101$, $a = 10$ cm, $f_o = 500$ Hz we have

$$x = Ka = nK_o a \simeq 10^{-4}$$

$$\Delta = \sqrt{in\omega_o \mu_o \mu_r/\sigma} \; / \; Z_o \qquad (5.3)$$

$$= (1 + i)A \simeq O(10^{-6}) \quad .$$

B_1 and C_1 of equation (2.25) could be approximated by

$$B_1 \simeq - \frac{\frac{2x}{3} - i\frac{x^2}{3}}{\frac{2x}{3} - \frac{i}{x^2} - i\Delta(\frac{x^2}{3} + \frac{i}{x})} \simeq \frac{-2}{3} x^3 \, i \qquad (5.4)$$

and

$$C_1 \simeq - \frac{\frac{2x}{3} - i\frac{x^2}{3}}{\Delta(\frac{2x}{3} - \frac{i}{x^2}) - i(\frac{x^2}{3} + \frac{i}{x})} \simeq - \frac{x^2}{3} (3A - ix) \qquad (5.5)$$

In particular, the scattering function $P(\theta)$ which is given by (2.25) can be shown to be (for back scattering at $\theta = \pi$)

$$Re[P(\pi)] = 1.5Ax^2 \qquad (5.6)$$

$$Im[P(\pi)] = -1.5 \, x^3 \qquad (5.7)$$

where Re and Im refer to the real and the imaginary part of $P(\pi)$. It is evident from (5.6) and (5.7) that, both x and A can be determined from the measurement of $P(\pi)$. Because, the dependence of $P(\pi)$ on A and x involves simple functions, evaluation of both x and A can be carried out for several harmonics. The measured data can be used to determine the average value for both 'a' and A, that is the sphere radius and its surface impedance. In utilizing the above expressions, calculations were made by using the computed scattered fields. It was found that equations (5.6) and (5.7) can yield the radius of the sphere and the surface impedance A, within an error limit of 5%. A sampled computation of the radius 'a' using several harmonics of the incident field are shown in Fig. 5.1. It is interesting to note that the computed values are always smaller than the actual values of a, and the computation error decreases somewhat as the order of the utilized harmonic increases. For a better approximation, one can compute the radius a using equation (5.7) and then utilizing the exact expression for the scattered field to determine A. This type of computation was found to give results to within an accuracy of 1%. Fig. 5.2 shows a sampled computation of A using several harmonics of the incident field.

5.2.2 Current Loop Excitation

In this section the near scattered field with low frequency approximation when an impedance sphere is excited by a uniform current loop is considered. In terms of $x1 = Ka$, $x2 = Kb$, $x3 = Kc$ and $\Delta = A(1+i)$, equation (3.32) can be rewritten in the form,

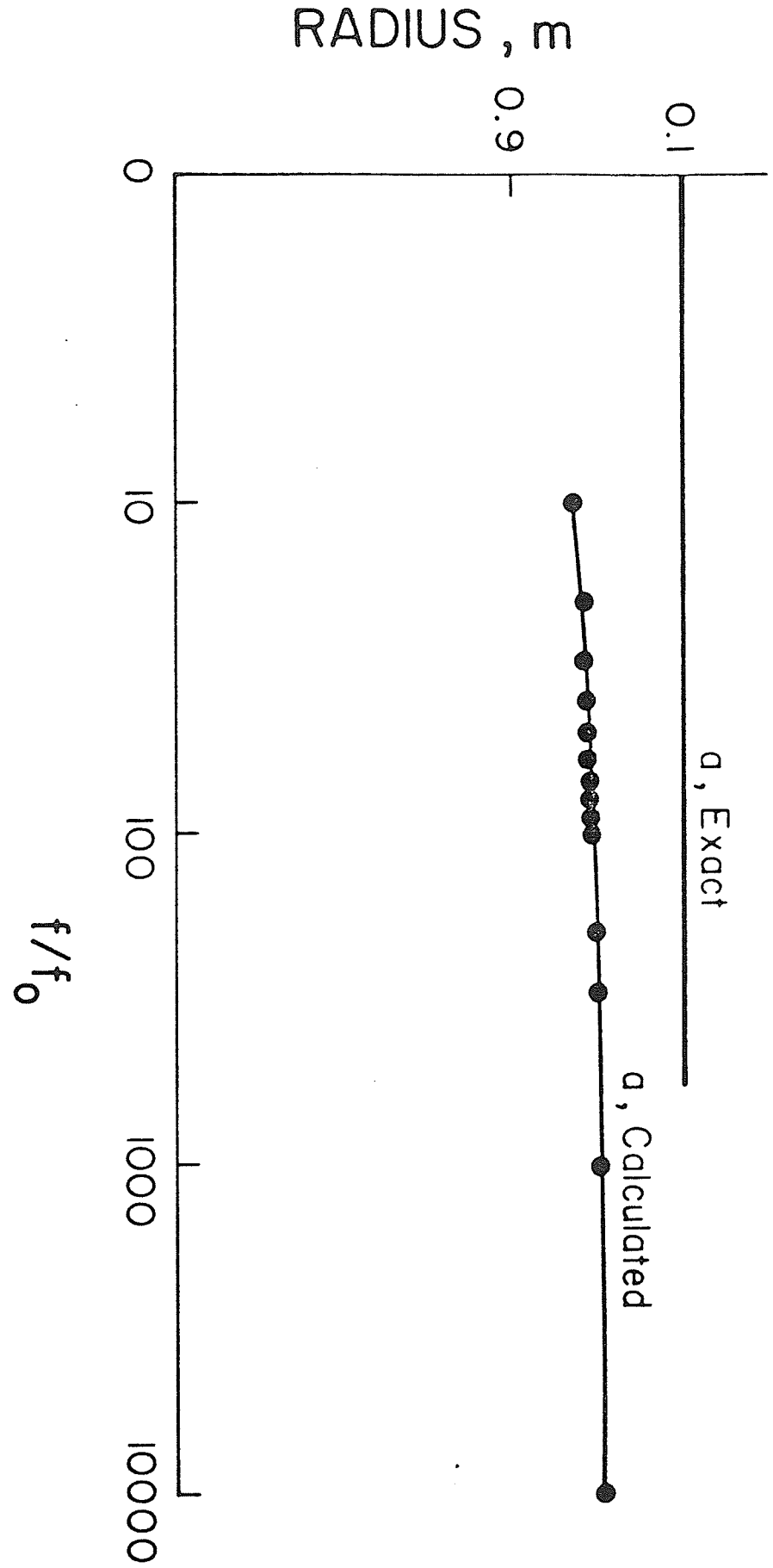

Fig. (5-1) Calculated radius of sphere.

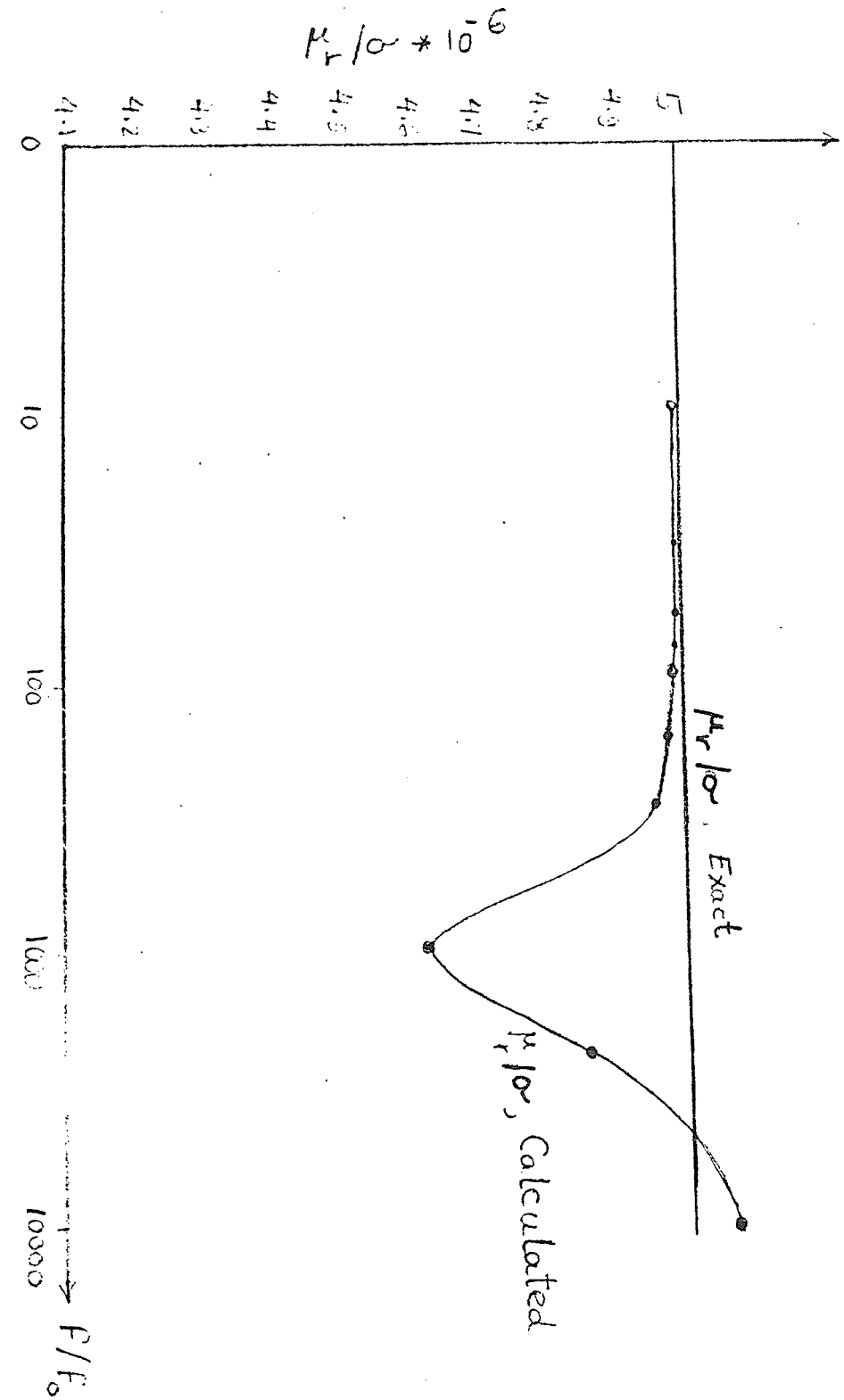

Fig. (5-2) Calculated electrical parameters of sphere.

$$\text{Re}[Q] = \frac{6\, x_1^3\, A}{x_2 x_3 (x_1 + 2A)} \tag{5.8}$$

$$\text{Im}[Q] = \frac{2\, x_1^3 (A - x_1)}{x_2 x_3 (x_1 + 2A)} \tag{5.9}$$

Dividing equations (5.8) to (5.9), we obtain

$$\frac{\text{Re}[Q]}{\text{Im}[Q]} = \frac{3A}{A - x_1} \tag{5.10}$$

Comparing these expressions with those of the plane wave incident on a sphere given in equations (5.6) and (5.7), we note that the approximation is poor in the present case. However, the nature of the expressions are similar. Provided x_2 and x_3 are known, (5.9) can be used to determine x_1 approximately under the condition $A \ll x_1$. The computed value of x_1 can then be used in (5.8) to determine A. Note that, in the present case of dipole excitation of a sphere, additional unknowns x_2 and x_3, i.e. b and c in Fig. 5.3, are introduced. It is obvious that using the radial magnetic field, the determination of all unknown parameters is not readily feasible. It may be possible to generate other independent expressions from the remaining field components to enable one to determine all unknown parameters. Instead, in the next section, the time response of an impedance sphere will be used to determine all the above unknown parameters.

5.3 Time Domain

In this section, the transient analysis of an impedance sphere excited by a uniform current loop is used to determine the unknown parameters a , b , c , a, and μ_r . Using equation (4.5) the transfer function

$$f_n(n\omega_o) = \frac{H_r^s}{H_r^i} \tag{5.11}$$

which maybe approximated at low frequency by

$$f_n(n\omega_o) = \frac{+a^2(c-b)^2}{b^3 c^2 K}(Ka + i\,3A) \tag{5.12}$$

i.e.

$$Re[f_n(n\omega_o)] = \frac{+a^3(c-b)^2}{b^3 c^2} \tag{5.13}$$

$$Im[f_n(n\omega_o)] = \frac{+3a^2(c-b)A}{b^3 c^2 K} \tag{5.14}$$

and

$$\frac{Re[f_n(n\omega_o)]}{Im[f_n(n\omega_o)]} = \frac{Ka}{3A} \tag{5.15}$$

Note that, again a can be obtained from (5.13) upon using the known values of b and c . In practice, both b and c are unknowns, however since (5.13) depends strongly on (c-b) , an approximate value for b and c can be obtained by either changing the height of both transmitter and receiver coils, or by modifying the separation of the two coils. However, equation (4.4) can be rewritten in the form

$$F(t) = \sum_{n=1}^{\infty} [A_n \, Re(f_n) \cos(n\omega_o t) - A_n I_m(f_n) \sin(n\omega_o t)] \quad \ldots (5.16)$$

from which we get

$$A_n Re(f_n(n\omega_o t)) = \frac{1}{T} \int_0^T F(t) \cos(n\omega_o t) dt \quad (5.17)$$

$$A_n I_m(f_n(n\omega_o t)) = \frac{-1}{T} \int_0^T F(t) \sin(n\omega_o t) dt \quad (5.18)$$

where

$$T = 2\pi/\omega_o \quad (5.19)$$

and $F(t)$ is the time response of the sphere. These equations can be utilized to obtain the required data from the time response in order to compute 'a' and A from (5.13) and (5.14). Because the transfer function $f_n(n\omega_o)$ depends on all geometrical parameters a, b, and c and the physical parameter A which is a function of σ and μ_r of the sphere, the time response is dependent on all these parameters as we discussed in Chapter Four. It, therefore, becomes evident that a knowledge of $F(t)$; i.e. the time response, is not sufficient to determine the parameters of the scatterer by using the above approximate expressions.

The above mentioned difficulties are obviated by solving the problem with a non-linear optimization routine. The particular optimization routine used in this work is called SIMPLEX [16], [17]. This subroutine finds the values of several independent variables

$\overline{X}$ such that a given function (called the objective function) $U(\overline{X})$ of these independent variables attains its minimum value.

The objective function we have used in this work has the form (the error function)

$$U = U(\overline{X},t_i) = \sqrt{\sum_{i=1}^{n} (F(X,t_i) - \phi(t_i))^2} \qquad (5.20)$$

where

$F(\overline{X},t)$ is the analytical time response,

$\overline{X}$ represents the unknown parameters,

t is an independent variable, e.g. time,

$\phi(t)$ is the measured time response.

In order for equation (5.20) to represent a physical phenomenon, there are certain restrictions on the unknown parameters in (5.16); e.g. they all must be real and positive. Incorporation of these restrictions into the optimization routine makes it possible to select the physical possible solution and reject all other solutions of (5.20).

The user must supply initial approximations to the values of the independent variables at the minimum, initial size of the simplex, expansion, reflection, contraction factors and a subroutine to evaluate the objective function for any values of the independent variables. The computer software for numerical solution consists of routines FIT, FIELD, and FUN . The subroutine FIT determines a function $y = \phi(t)$ which is satisfied by our sets of measured values (y_1, t_1), (y_2, t_2) , etc, and which allows us to infer reasonable values of y for other values of t , where we have no measurement.

Least-square curve fitting method is used and the total interval T is divided into subintervals $T_1, T_2, \ldots, T_\ell$, for each of which $\phi_i(t)$ has the form $\beta_i \exp(-\alpha_i t)$, $t \in T_i$ and $i = 1, 2, \ldots, \ell$. Fig. 5.4 shows a an example of the interval divisions for an available data measured by DRES.

The subroutine FIELD uses equation (5.16) to calculate the time response of the scattered field from a sphere by using the impedance boundary conditions. FUN generates the objective function $U(\overline{X}, t)$.

Application of the software described on impedance sphere with the available measured data by DRES results in the following values:

$\mu_r = 50$

$\sigma = 10^7$ mhos

b = 10. cm.

a = 0.5 cm

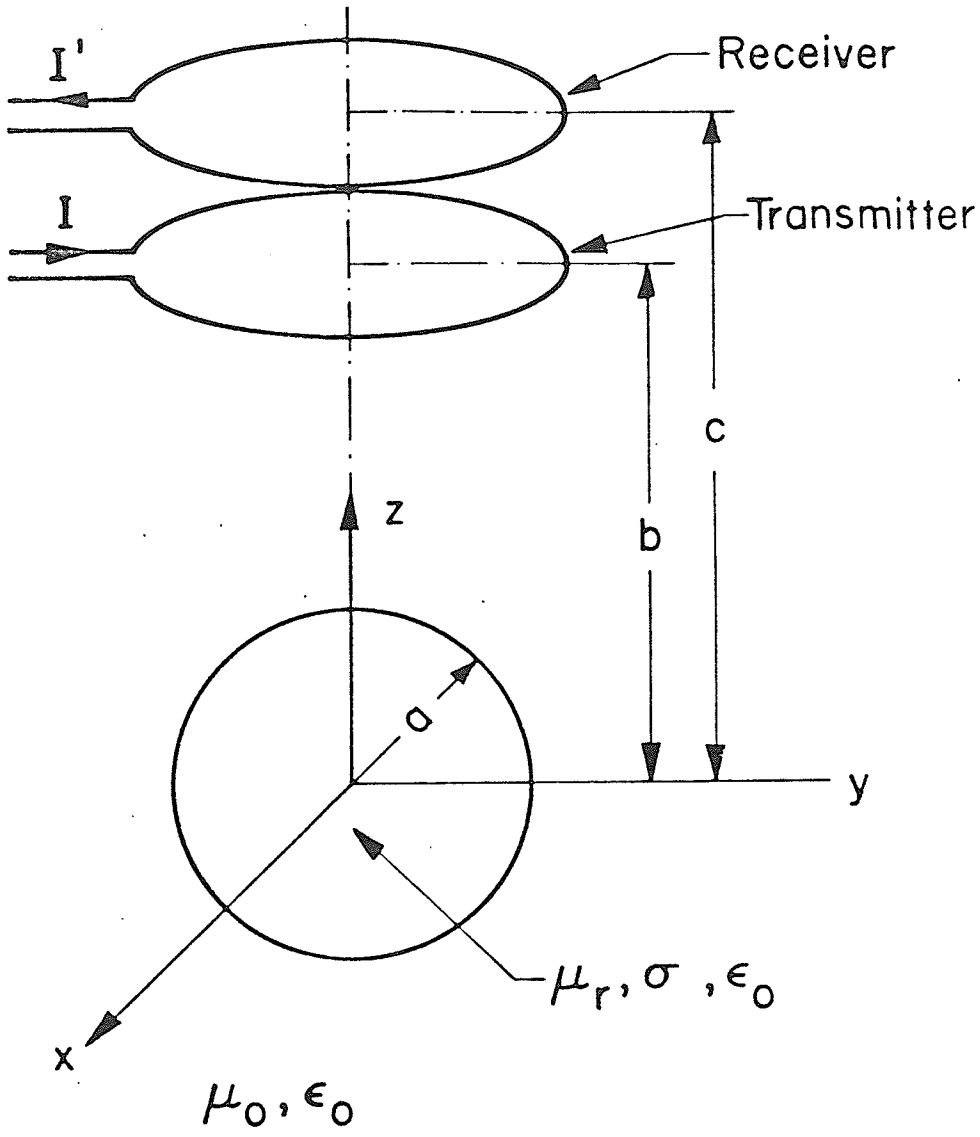

Fig. 5-3 Geometry of sphere excitation.

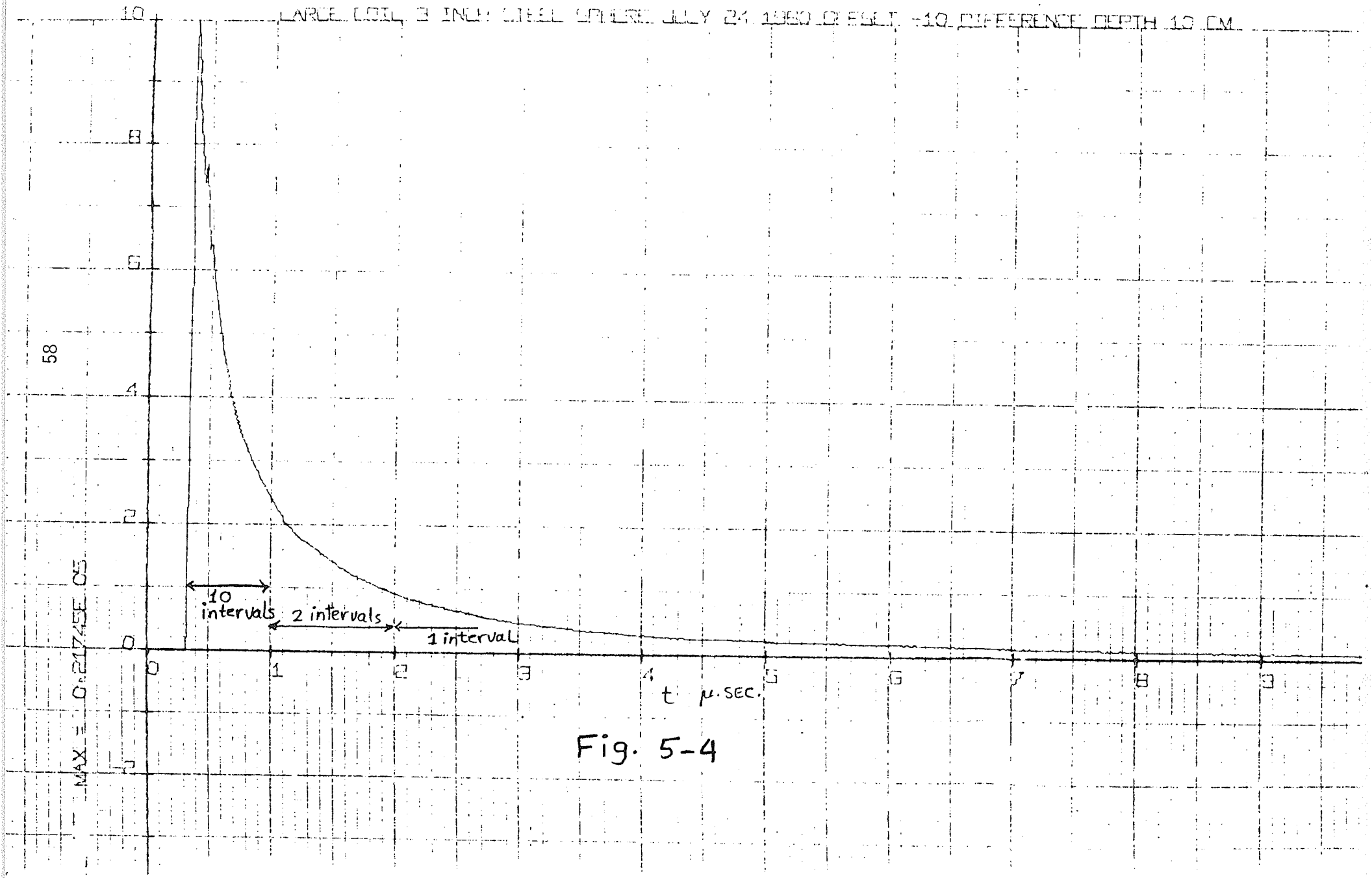
LARGE COIL 3 INCH STEEL SPHERE JULY 24 1960 0 FEET -10 DIFFERENCE DEPTH 10 CM
10
8
6
4
2
0
58
MAX = 0.21745E 05
10 intervals
2 intervals
1 interval
0
1
2
3
4
5
6
7
8
9
t μ.sec.

Fig. 5-4

CHAPTER SIX

CONCLUSIONS

In this thesis the problem of electromagnetic scattering from a highly conducting permeable sphere was used to study both the frequency and the time domain response; using a method based on Impedance Boundary Condition (IBC). The method is justified by the fact that, at low frequencies of operation the signal penetration into the sphere is small and a solution based on the surface properties of the scatterer is a reasonable one. It is hoped that this study of an old problem from a viewpoint different than previous appraches will be of value in improving our knowledge of the phenomena involved. Solutions are presented for the electromagnetic field scattered by a sphere of arbitrary surface impedance for both plane wave and dipole source excitations. For a Lossy dielectric sphere, good agreement between the solution based on IBC method and that based on the classical method of the continuity of fields at the surface of the sphere is obtained.

The low frequency approximation is used for the two types of excitations to simplify solutions in the frequency domain. This simplification is done by using proper approximation to the Bessel and the Hankel functions. A simple approach for determining the sphere parameters (i.e. the sphere radius and its electrical parameters) is introduced. The result is useful for determining the size of the spherical targets and for estimating their parameters. Generally the IBC method is also applied for any imperfectly conducting arbitrary-shaped body provided that:

a) The skin depth is very small compared with the radius of

curvature of the body and the wave length.

b) The radius of curvature is large compared with respect to the wave length.

c) The surface impedance of the body relative to the free space, which is given by $\Delta = Z/Z_0$, has a magnitude very small compared to unity.

Using the frequency domain solution the time domain solution is also computed. For a pulse train incident field, it is found that the time response behaviour depends strongly on all parameters involved. Thus a determination of the sphere parameters from a single time response data may not be, in general, feasible. However by using non-linear optimization techniques one can determine the sphere parameters by minimizing the difference between the scattered field evaluated by the IBC and that measured by an experimental system.

To conclude, further research is still needed to evaluate the usefulness of IBC for solutions of scattering problems for other objects. An important area of research would involve the extension of this method for time domain problems. Currently, we are working towards the application of IBC for investigation of time response of impedance prolate spheroids.

REFERENCES

[1] Stratton, J.A. (1941), Electromagnetic Theory, McGraw-Hill Book Co., Inc., New York.

[2] Garbacz, R.J. (1964), Bistatic scattering from a class of lossy dielectric spheres with surface impedance boundary conditions, Phys. Rev. 133, A14-A16.

[3] Wait, J.R. (1963), Electromagnetic scattering from a radially inhomogeneous sphere, App. Sci. Res. 10, Sec. B.

[4] Wait, J.R. and C.M. Jackson (1965), Calculations of the bistatic scattering cross section of a sphere with an impedance boundary condition, Rad. Sci. Jor. of Res., Vol. 69D, No. 2.

[5] Senior, T.B.A. (1961), Impedance boundary condition for imperfectly conducting surfaces, Appl. Sci. Res., Vol. 8, Sec. B.

[6] Mitzner, K.M. (1967), An integral equation approach to scattering from a body of finite conductivity, Rad. Sci., Vol. 2 (New Series) No. 12.

[7] Wait, J.R. (1962), Electromagnetic waves in stratified media, Pergamon Press, Oxford.

[8] Harrington, R.F. (1961), Time harmonic electromagnetic fields, McGraw-Hill Book Co., Inc., New York.

[9] Abramowitz, M. and I.A. Stegum (Editors, 1964), Handbook of mathematical functions, National Bureau of Standards, A.M.S. 55.

[10] Kennaugh, E.M. and R.L. Cosgriff (1958), The use of impulse response in electromagnetic scattering problems, IRE Nat. Conv. Rec., Pt. 1.

[11] Kennaugh, E.M. (1961), The scattering of short electromagnetic

pulses by a conducting sphere, Proc. of the IRE, Vol. 48.

[12] Weston, V.H., Pulse return from a sphere, IRE Trans. and Prop., Vol. AP-7.

[13] Rheinstein, J. (1968), Scattering of short pulses of electromagnetic waves, IEEE, AP 16.

[14] Hill, D.A. and J.R. Wait (1972), The transient electromagnetic response of a spherical shell of arbitrary thickness, Rad. Sci., Vol. 7, No. 10.

[15] Felsen, L.B. (Editor, 1976), Transient electromagnetic Fields, Springer-Verlay, New York.

[16] Nelder, J.A. and R. Mead (1965), A simplex method for function minimization, The Comp. Jor., 7.

[17] Walsh, G.R. (1975), Methods of optimization, A Wiley - Interscience Publication, New York.

[18] Shafai, L., A. Mohsen and A. Sepak (1980), Time response of conducting permeable sphere, Final Report, Contract 8SU79- 00243, E.E. Dept., University of Manitoba, Ch. 2.

APPENDIX A

APPROXIMATION OF EQUATION (2.25)

In the scattered function $P(\theta)$ which is given by

$$P(\theta) = \sum_{n=1,2,\ldots} \frac{2n+1}{n(n+1)} \left(B_n \frac{d}{d\theta}\left(P_n^1(\cos\theta)\right) + C_n \frac{P_n^1(\cos\theta)}{\sin\theta}\right) \quad \text{(A-1)}$$

the $n=1$ term becomes dominant for small Ka. Hence, for highly conducting sphere at low frequencies we have

$$P(\theta) = \frac{-3}{2}\left(B_1 \cos\theta + C_1\right) \quad \text{(A-2)}$$

where

$$B_1 = -\frac{\hat{J}_1'(Ka) - i\Delta\,\hat{J}_1(Ka)}{\hat{H}_1^{(2)'} - i\Delta\hat{H}_1^{(2)}(Ka)}$$
$$C_1 = \frac{\Delta\,\hat{J}_1'(Ka) - i\,\hat{J}_1(Ka)}{\Delta\,\hat{H}_1^{(2)'}(Ka) - i\,\hat{H}_1^{(2)}(Ka)} \quad \text{(A-3)}$$

Using small-argument approximation for the spherical Bessel function and using

$$= A(1+i) \quad \text{where} \quad A = \frac{\omega\mu}{2\sigma}/Z_o \quad , \quad \text{we have}$$

$$B_1 = -\frac{\frac{2\,Ka}{3} - i(1+i)A\frac{(Ka)^2}{3}}{\frac{2\,Ka}{3} - \frac{1}{(Ka)^2} - i(1+i)A\left(\frac{(Ka)^2}{3} + \frac{i}{Ka}\right)} \quad \text{(A-4)}$$

for highly conducting spheres of radii in the range of 0.1 - 1 meter and at a frequency of 500 Hz

$$Ka = O(10^{-4})$$

$$A = O(10^{-7})$$

Therefore, one can neglect A w.r.t Ka in (A-4), which gives

$$B_1 = \frac{-2}{3} (Ka)^3 \, i \qquad \text{(A-5)}$$

and

$$C_1 = \frac{-1}{3}(Ka)^3 \, (3A - iKa) \qquad \text{(A-6)}$$

APPENDIX B

APPROXIMATION OF EQUATION (3.3.2)

In the scattered function $Q(\ )$ which is given by

$$Q(\theta) = \sum_{n=1,2,\ldots} n(n+1)(2n+1)\hat{H}_n^{(2)}(Kb)\hat{H}_n^{(2)'}(Kc)P_n'(\cos\theta) \cdot \frac{\hat{J}_n'(Ka) - i\Delta\hat{J}_n(Ka)}{\hat{H}_n^{(2)'}(Ka) - i\Delta\hat{H}_n^{(2)}(Ka)}$$

the $n=1$ term becomes dominant at low frequencies.

Putting $x_1 = Ka$, $x_2 = Kb$, $x_3 = Kc$ and $\Delta = (1+i)A$, and using small argument formula for the spherical Bessel function, we have

$$Q(\theta) = \sigma\left(\frac{-1}{x_2x_3} + i\ \frac{x_2^3 + x_3^3}{3x_2x_3}\right)(-1)\left(\frac{x_1^3}{3} \cdot \frac{3A + i(A-x_1)}{x_1 + 2A}\right)$$

$$\simeq \frac{\sigma\, x_1^3}{3x_2x_3(x_1+2A)}\ (-3 + 0)(-1)\left(\frac{3A + i(A-x_1)}{3}\right)$$

$$\simeq \frac{2\, x_1^3}{x_2x_3(x_1+2A)}\ (3A + i(A-x_1))$$

APPENDIX C

DERIVATION OF EQUATION (4.3)

For Z directed electric dipole of moment $I\ell$ and of arbitrary location, Harrington [8] has shown that the magnetic vector potential A_z is given by

$$A_z = \frac{I\ell}{4\pi} \frac{e^{-ik|r-r'|}}{|r-r'|} \tag{C-1}$$

Similarly for a magnetic dipole of moment ML , the electric vector potential F_z is given by

$$F_z = \frac{ML}{4\pi} \frac{e^{-ik|r-r'|}}{|r-r'|} \tag{C-2}$$

The electromagnetic field of the magnetic dipole is obtained by using the relations

$$E = -\nabla \times F$$

and

$$H = \frac{1}{i\omega\mu} \nabla \times \nabla \times F \tag{C-3}$$

Since $F_r = F_z \cos\theta$

and

$$F_\theta = -F_z \sin\theta \tag{C-4}$$

Therefore

$$\nabla \times F|_{\theta} = 0$$

$$\nabla \times F|_{r} = 0$$

$$\nabla \times F|_{\phi} = \frac{1}{r}\left(\frac{\partial}{\partial r}(r F_{\theta}) - \frac{\partial F_r}{\partial \theta}\right) = W(r,\theta) \qquad \text{(C-5)}$$

Also

$$\nabla \times \nabla \times F|_{\phi} = 0$$

$$\nabla \times \nabla \times F|_{\theta} = \frac{-1}{r}\frac{\partial}{\partial r}(rW)$$

$$\nabla \times \nabla \times F|_{r} = \frac{1}{r\sin\theta}\frac{\partial}{\partial \theta}(W \sin\theta) \qquad \text{(C-6)}$$

where

$$W(r,\theta) = \frac{-1}{r}\left(r\sin\theta \frac{\partial F_z}{\partial r}\right) \qquad \text{(C-7)}$$

$$H_r = \frac{1}{i\omega\mu}(\nabla \times \nabla \times F)_r$$

$$= \frac{1}{i\omega\mu}\frac{1}{r\sin\theta}\frac{\partial}{\partial \theta}(W \sin\theta)$$

$$= \frac{1}{i\omega\mu r}\left(-2\cos\theta \frac{\partial F_z}{\partial r}\right) \qquad \text{(C-8)}$$

For $\theta = \pi$ we have

$$H_r = \frac{(ML)}{2i\pi\omega\mu r}\left(\frac{-ik|r-r'|-1}{|r-r'|}\right)\exp(-ik|r-r'|) \qquad \text{(C-9)}$$